PATIENT-SPECIFIC EPILEPTIC SEIZURE ONSET DETECTION VIA FUSED EEG AND ECG SIGNALS

A Dissertation

by

MARWA KHALID QARAQE

Submitted to the Office of Graduate and Professional Studies of
Texas A&M University
in partial fulfillment of the requirements for the degree of

DOCTOR OF PHILOSOPHY

Chair of Committee,	Erchin Serpedin
Co-Chair of Committee,	Hazem Numan Nounou
Committee Members,	Mahmoud El-Halwagi
	Aydin Karsilayan
Head of Department,	Miroslav Begovic

May 2016

Major Subject: Electrical Engineering

ABSTRACT

Epilepsy is a neurological disorder that is associated with sudden and recurrent seizures. Epilepsy affects 65 million people world-wide and is the third most common neurological disorder, after stroke and Alzheimer disease. During an epileptic seizure, the brain endures a transient period of abnormally excessive synchronous activity, leading to a state of havoc for many epileptic patients. Seizures can range from being mild and unnoticeable to extremely violent and life threating. Many epileptic individuals are not able to control their seizures with any form of treatment or therapy. These individuals often experience serious risk of injury, limited independence and mobility, and social isolation.

In an attempt to increase the quality of life of epileptic individuals, much research has been dedicated to developing seizure onset detection systems that are capable of accurately and rapidly detecting signs of seizures. This thesis presents a novel seizure onset detection system that is based on the fusion of independent electroencephalogram (EEG) and electrocardiogram (ECG) based decisions. The EEG-based detector relies on a on a common spatial pattern (CSP)-based feature enhancement stage that enables better discrimination between seizure and non-seizure features. The EEG-based detector also introduces a novel classification system that uses logical operators to pool support vector machine (SVM) seizure onset detections made independently across different relevant EEG spectral bands. In the ECG-based detector, heart rate variability (HRV) is extracted and analyzed using a Matching-Pursuit and Wigner-Ville Distribution algorithm in order to effectively extract meaningful HRV features representative of seizure and non-seizure states. Two fusion systems are adopted to fuse the EEG- and ECG-based decisions. In the first system, EEG- and ECG-based

decisions are directly fused to obtain a final decision. The second fusion system adopts an over-ride option that allows for the EEG-based decision to over-ride the fusion-based decision in an event that the detector observes a string of EEG-based seizure decisions. The proposed detectors exhibit an improved performance, with respect to sensitivity and detection latency, compared with the state-of-the-art detectors. Experimental results demonstrate that the second detector achieves a sensitivity of 100%, detection latency of 2.6 seconds, and a specificity of 99.91% for the MAJORITY fusion case.

In addition, a novel method to calculate the amount of neural synchrony that exists between the channels of an EEG matrix is carried out. This method is based on extracting the condition number from multi-channel EEG at a particular time instant to indicate the level of neural synchrony at that particular time instant. The proposed method of neural synchrony calculation is implemented in two detection systems. The first system uses only neural synchrony as the feature for seizure classification whereas the second system fuses energy and synchrony based decision to make a final classification decision. Both systems show promising results when tested on a set of clinical patients.

DEDICATION

To Her Highness Sheikha Moza bint Nasser Al-Missned

and

to my Beloved Parents.

ACKNOWLEDGEMENTS

First and foremost, praise is due to Allah, the most gracious and most merciful. Without His guidance and blessing, my work would never have been possible.

I would like to acknowledge several people who provided advice, support, and encouragement to me throughout the completion of this thesis. I would like to express my deepest respect and gratitude to my advisor, Dr. Erchin Serpedin, for his wonderful guidance and support over the years. His deep insight, vast knowledge, and patience have been crucial for the completion of my thesis. I would also like to express my appreciation to my co-chair, Dr. Hazem Nounou, for his valuable mentoring and constant support.

I am deeply and forever indebted to my parents for their love, support, and encouragement throughout my life. I congratulate them for this thesis; for in reality, this work is partly theirs as well. I would also like to thank my sisters and brother for their constant encouragement throughout my journey. I am also very thankful for my husband for his help, love, and support throughout the toughest times.

In addition, I would like to express my gratitude to Dr. Muhammad Ismail for his support and guidance. It is greatly appreciated. I am also thankful for Dr. Qammer Abassi for his support. In addition, I would like to express my appreciation to my committee members, Dr. Mahmoud El-Halwagi and Dr. Aydin Karsilayan, for serving on my committee and for their valuable feedback throughout the completion of my thesis work. Also, many thanks are due to Dr. Zulfi Haneef for teaching me about epilepsy and for providing me with clinical data from his patients.

Furthermore, I would like to thank Her Highness Sheikha Moza bint Nasser Al-Missned, Chairperson of Qatar Foundation for Education, Science, and Community

Development, for her constant support in promoting education and being a driving force in the success of Qatar Foundation. I would like to also express my appreciation to Dr. Ayman Bassil for his encouragement and support from the very beginning. I am also grateful for my sponsor, Qatar Foundation Science Leadership Program, for their sponsorship and assistance throughout my journey.

Much appreciation goes to Tammy Carda for her friendship, support, and help throughout it all. The ECEN Department is privileged to have a person like her helping its students.

NOMENCLATURE

AF	Always Fuse
ANN	Artificial Neural Network
BEADS	Baseline Estimation and Denoising with Sparsity
bps	Beast per Second
BS	Band-Sensitive Classification
CHB	Childrens' Hospital Boston
CN	Condition Number
CP	Complex Partial
CSP	Common Spatial Pattern
DL	Detection Latency
ECG	Electrocardiogram
ECoG	Electrocorticography
EEG	Electroencephalographic
EMG	Electromyogram
EOG	Electrooculography
EWSA	Equal Weight Spatial Averaging
FA	False Alarm
FDA	Food and Drug Administration
fMRI	Function Magnetic Resonance Imaging
GS	Generalized Seizure
HR	Heart Rate
HRV	Heart Rate Variability
IED	Ictal Epileptiform Discharge

iEEG	Intracranial Electroencephalographic
IHR	Instantaneous Heart Rate
ITC	Ictal Tachycardia
ITC	Ictal Tachycardia
MAJ	Majority
MP	Matching Pursuit
OF	Over-ride Fuse
PWVD	pseudo-WVD
RBF	Radial Basis Function
S	Sensitivity
SOD	Seizure Onset Detector
SP	Simple Partial
SPECT	Single Photon Emission Computed Tomography
SPWVD	smoothed-pseudo-WVD
SUDEP	Sudden Unexpected Death in Epileptic Patients
SVD	Singular Value Decomposition
SVM	Support Vector Machine
TC	Traditional Classification
TF	Time-Frequency
TLE	Temporal Lobe Epilepsy
VNS	Vagus Nerve Simulator
WVD	Wigner-Ville Distribution

TABLE OF CONTENTS

Page

LIST OF FIGURES

FIGURE Page

LIST OF TABLES

TABLE Page

1. INTRODUCTION

This chapter describes the essential background material about the neurological disorder of epilepsy, its treatment, and research that has been done in this area to help alleviate its symptoms. In this chapter, the shortcomings of existing works in the area of epilepsy detection are outlined and the contributions brought by this thesis are summarized.

1.1 Epilepsy

Epilepsy is a neurological disorder which affects the nervous system and is associated with recurrent seizures. Epileptic seizures are caused by disturbances in the electrical activity of the brain. During a seizure, the brain endures a transient period of abnormal excessive or synchronous neural activity. This sudden breakdown of neural activity of the brain can be disastrous to the patient, forcing the patient to endure involuntary alterations in behavior, movement, sensation, or consciousness [1], [2].

The underlying genetic and molecular mechanisms that give rise to epilepsy is still poorly understood; however, epilepsy has distinctive characteristics differentiating it from non-epileptic seizures. Epilepsy is defined as (1) at least two unprovoked seizures occurring at least 24 hours apart, (2) one unprovoked seizure with a high likelihood of recurrent unprovoked seizures, or (3) diagnosis of an epilepsy syndrome [3]. Non-epileptic seizures are a response to disturbances external to the central nervous system, such as alcohol, drug abuse, sleep deprivation, or an acute illness. Epilepsy is conceptually divided by etiology into the following categories [3]:

1. **Genetic**: most likely due to genetic predisposition.

2. **Structural/Metabolic**: due to a lesion in the brain.

3. **Unknown**: no identifiable focus or syndrome.

Identifying the underlying cause of epilepsy is important because it helps in determining the type of anti-seizure medication that should be tried. Unfortunately, at present, six out of ten patients are diagnosed with epilepsy with the cause of it remaining unknown.

1.1.1 Types of Seizures and their Symptoms

Epileptic seizures can be divided into two major categories: partial seizures and generalized seizures. Partial seizures are characterized by an epileptic activity that begins and remains localized in one part of the brain. Partial seizures can be further divided into two classes: namely, simple partial seizures and complex partial seizures. Simple partial seizures do not alter consciousness, but do temporary impair an individual's sensory system if the epileptic activity originates from the somatosensory area of the brain, and the motor systems if the epileptic activity originates from the motor cortex. During a simple partial *sensory* seizure, an individual may experience somatosensory, autonomic, or psychic symptoms. Some of the somatosensory symptoms include hallucinations, altered vision, speech, and smell. Autonomic symptoms include sweating and papillary dilation, and psychic symptoms can include a sudden sensation of fear, anger, dreamy states, auras, and deja vu. Symptoms of simple partial sensory seizures are typically very subtle and can be difficult to distinguish from psychological phenomenas. However, simple partial *motor* seizures are characterized by much clearer clinical manifestations, such as rapid muscular contractions on one side of the body and postural movements. Simple partial seizures usually last for a minute or less and the individual is able to remember what happened after the seizure passes. During a complex partial seizure, an individual's consciousness

is compromised. These seizures usually start in a small area of the temporal lobe or frontal lobe of the brain and quickly involve other areas of the brain that affect alertness and awareness. These seizures are often preceded by auras and automatism (snapping fingers, picking at things, walking aimlessly, lip smacking, or mumbling). Complex partial seizures typically last between one to three minutes and individuals might experiences a sense of confusion after the seizures pass.

The second category of epileptic seizures is referred to as generalized seizures. These types of seizures involve the entire brain from the onset. Generalized seizures that include convulsions are called generalized convulsive seizures and those that do not assume convulsions are classified as generalized non-convulsive seizures. Generalized convulsive seizures can be further subdivided into the following classes:

- **Myoclonic seizures**: result in rapid convulsions but do not typically alter an individual's state of consciousness.
- **Clonic seizures**: result in convulsions and loss of consciousness.
- **Tonic seizures**: result in sudden contraction of truncal and facial muscles accompanied by sudden stiffening movements of the arms or legs. These types of seizures usually lead to serious injuries due to sudden and dangerous falls.
- **Tonic-clonic seizures**: combine the clinical manifestation of tonic and clonic seizures and begin without warning. These seizures usually last between one to two minutes but individuals may not regain consciousness until ten to fifteen minutes after the seizures. They may also experience fatigue for hours or days.

Generalized non-convulsive seizures can be divided into two sub-classes, those that lead to loss of consciousness and those that do not. Generalized non-convulsive

seizures that lead to loss of consciousness are called absence seizures and are associated with involuntary eye blinking, staring, and other minor facial movements. These seizures typically last between a few seconds and a minute, and can occur many times throughout the day. Atonic seizures are generalized non-convulsive seizures that do not lead to a loss of consciousness; however, they do lead to a sudden loss of tone in postural muscles which leads to serious injuries from dangerous falls [2].

1.1.2 Treatment of Epilepsy

Epilepsy affects individuals with a different degree of severity; thus, the treatment of epilepsy is patient-specific. The first course of treatment for epileptic individuals is with the use of anti-epileptic drugs. Approximately 70-80% of epileptic patients are able to limit their seizures, the severity of the seizures, and their frequency through anti-epileptic drugs. These drugs essentially limit the capacity of neurons to fire at excessive rates. Between 20-30% of epileptic patients suffer from a condition called refractory epilepsy where they do not respond to any form of medication. As a result, these patients resort to different treatments options, such as surgery, vagus nerve stimulation, and ketogenic diets.

Surgery is a possible option for some individuals once a team of epileptologists can accurately identify the region of the brain from which the abnormal neural firings originate from. This is accomplished by combining clinical, electrographic, anatomical, functional, and metabolic evidence from different forms of testing and procedures. Once the epileptogenic focus of the brain has been identified and it has been confirmed that the removal of that area of the brain will not lead to serious repercussions, the patient undergoes brain surgery.

Patients that are not surgical candidates may respond to vagus nerve stimulation (VNS) therapy. This treatment option involves implanting an electronic device which

is designed to prevent seizures by sending regular, mild pulses of electrical energy to the brain via the vagus nerve on the left side of the neck. The vagus nerve is part of the autonomic nervous system which controls functions of the body that are not under voluntary control, such as heart rate. The vagus nerve passes through the neck as it travels between the chest and abdomen and the lower part of the brain. The vagus nerve stimulator is programmed to send a stimulation signal to the brain at set intervals to neutralize any abnormal neural firings. VNS has been found to control seizures and relieve some side effects. Holding a special magnet near the implanted device triggers the device to deliver another burst of stimulation, outside of the programmed intervals. For people with warnings (auras) before their seizures, activating the stimulator with the magnet when the warning occurs may help to prevent the seizure.

The ketogenic diet is a high fat, average protein, low carbohydrate diet that has shown to be effective in controlling some patients' seizures. The diet forces the body to go into a ketosis state, in which it uses ketones (from fats) rather than glucose (from carbohydrates) for energy. The exact mechanisms which allow this diet to reduce frequency and severity of seizures is still unknown [4].

1.2 Manifestation of Epilepsy in Biosignals

The manifestation of epilepsy is a fairly complex procedure. In order to gain more insight on how epilepsy develops, doctors often monitor various biosignals of a patient for answers. Electrical biosignals are the most common continuous-time signals studied. Electrical biosignals refer to changes in the electric current produced by the sum of an electrical potential difference across a specialized tissue, organ, or cell system. Among the most common are electroencephalogram (EEG), which refers to the recording of electrical activity of the brain, electrocardiogram (ECG), which

represents the recording of electrical activity of the heart, electromyogram (EMG), which captures the electrical activity produced by skeletal muscles, and electrooculography (EOG), which measures the corneo-retinal standing potential that exists between the front and the back of the human eye. The most informative biosignals in terms of studying the manifestation of epileptic seizures in the human body are EEG and ECG.

1.2.1 EEG

The EEG is an electrophysiological monitoring method that records the electrical activity of the cerebral cortex through the use of electrodes that are placed either along the scalp or surgically placed on the exposed surface of the brain, methods that are referred to as electrocorticography (ECoG) and intracranial EEG (iEEG), respectively. In scalp EEG, electrodes are symmetrically arrayed on the scalp according to the International 10-20 system, shown in Figure 1.1. This system is an internationally recognized method to describe and apply scalp electrodes for EEG recording and ensures standardized reproducibility so that a subject's studies can be compared over time and subjects can be compared to each other.

Figure 1.2 illustrates the placement of the EEG on a patient. An EEG channel/signal is formed by taking the difference between the potentials measured at two electrodes. Each EEG channel summarizes activity localized within that region of the brain. EEG has many advantages including low hardware costs, tolerance to subject movement, and noislessness. EEG does not involve exposure to radioligands and is also a powerful tool for tracking brain changes. However, there are some disadvantages associated with EEG. These disadvantages include low spatial resolution on the scalp, poor measurement of neural activity under the cerebral cortex, artifacts, and very low signal-to-noise power ration. Therefore, robust data analysis

techniques are needed to extract meaningful information.

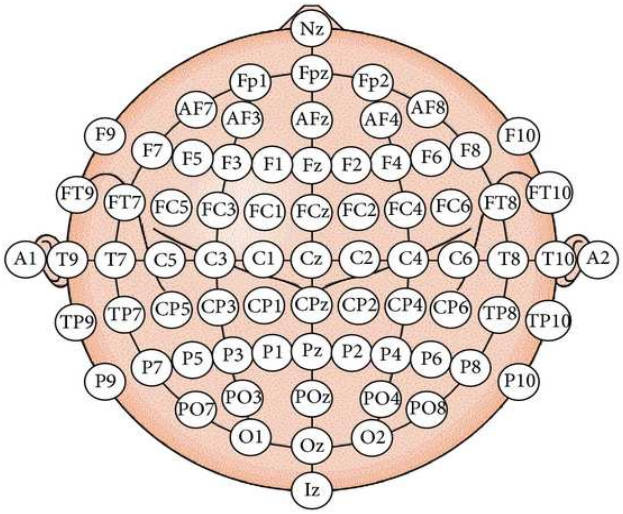

Figure 1.1: International 10-20 system for placement of scalp EEG electrodes [5].

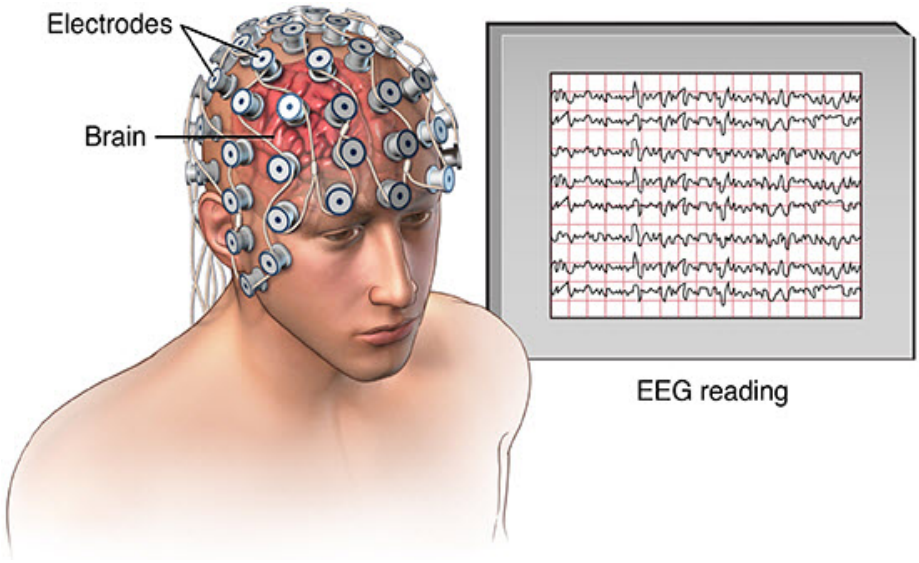

Figure 1.2: Illustration of the EEG on a human subject [6].

Expert electroencephalographers describe EEG activity in terms of its spatial distribution on the scalp and its dominant frequency component. The EEG activity of clinical relevance is limited to the frequency band $0.5 - 50$ Hz; however, the frequency range that captures various seizure onset electrographic manifestations is $0.5 - 25$ Hz. The sub-band signals that collectively represent the activity at time-scales corresponding to the seizure frequencies are the δ, θ, α, and β EEG frequency bands, where $\delta < 4$ Hz, $\theta \in [4, 7]$ Hz, $\alpha \in [8, 15]$ Hz, and $\beta \in [16, 31]$ Hz [7]. An illustration of the various EEG frequency band waveforms is given in Figure 1.3.

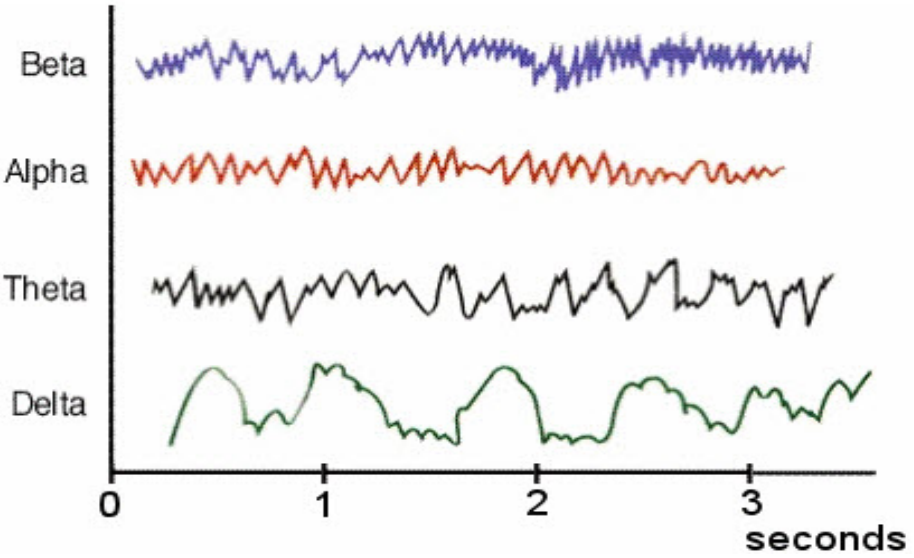

Figure 1.3: Illustration of the δ, θ, α, and β EEG frequency waveforms [8].

1.2.2 ECG

The ECG refers to the recording of electrical activity of the heart. The ECG is carried out by using electrodes placed on the body, which detect the electrical changes on the skin that arise from the heart muscle depolarization during each

heartbeat. With each heartbeat, an electrical impulse (wave) travels through the heart. This wave causes the muscle to squeeze and pump blood from the heart to the rest of the body. The right and left atria (upper chambers) create the first wave (P wave). When the electrical impulse travels to the bottom chambers, a flat line appears on the ECG. The right and left bottom chambers create the QRS complex. The final wave (T wave) represents the heart's electrical recovery in which it returns to a resting state. Figure 1.4 shows an illustration of a typical ECG waveform and Figure 1.5 illustrates the ECG placement on a patient.

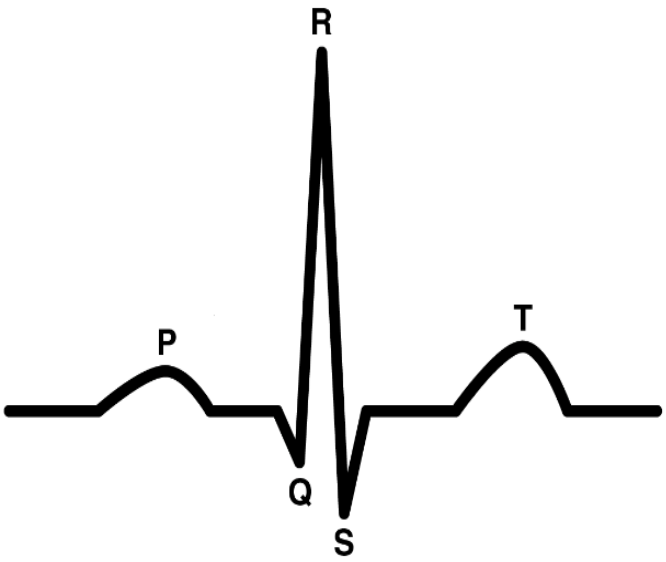

Figure 1.4: Illustration of the shape of the ECG [9].

Heart rate variability (HRV) is defined as the change in the heart's beat-to-beat interval and is often used in the analysis of cardiovascular regulatory mechanisms. However, recent advancements in the analysis of HRV in epilepsy reveal that epileptic seizures are accompanied by changes in various autonomic functions such as heart rate (HR) and in the same time unravel causes for sudden unexpected death in

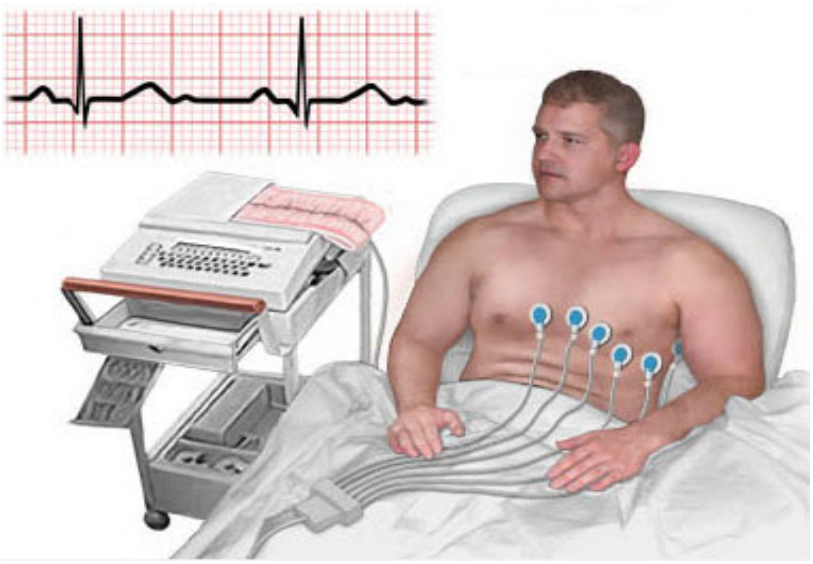

Figure 1.5: Illustration of the recording of the ECG on a human subject [10].

epileptic patients (SUDEP) [11], [12]. Furthermore, the estimation of the HRV before, during, and after a seizure provides an indication of the sum of sympathetic and parasympathetic inputs to the heart. Recent investigation points out that epilepsy is frequently associated with ictal tachycardia (ITC) or bradycardia, which, in some cases, precedes the onset of seizures [13].

1.3 Motivation of Research

Epilepsy affects 65 million people world-wide and approximately 3 million of those affected by epilepsy are in the United States. It is expected that 1 in 26 people in the United States will develop epilepsy at some point in their life. Epileptic patients whose treatment options have failed are forced to live a tough life. Their quality of life is severely limited. Many patients suffer serious injuries that include fractures, head injuries, and burns due to the sudden nature of the seizure attack along with the confusion, loss of consciousness, and lack of muscle control that accompanies certain types of seizures. These injuries account for a significant component of the

risk associated with epilepsy [14]. Furthermore, epileptic patients are unable to lead normal lives due to the disabling aspects of epilepsy. For example, many people are not able to drive, take care of babies, or carryout everyday activities that otherwise they would be able to do. Many patients also start to face emotional and physiological problems due to their illness.

In an attempt to increase the quality-of-life of epileptic patients, much research has been dedicated to developing a device that can detect the onset of seizure episodes before they happen. Such a device is called a seizure onset detector (SOD). SODs have many benefits. For instance, SODs can be used as warning devices to alert patients of imminent seizures so that the patient can take precaution measures before the seizure attack happens, and thus prevent serious injuries to themselves and those around them. In addition, SODs are gaining more attention as possible seizure control devices. Such detectors can control seizures by initiating anti-epileptic drugs or by selectively stimulating certain parts of the brain when an oncoming seizure is detected [15]. In a hospital setting, such a device would be useful in initiating time-sensitive clinical procedures necessary for the investigation of various epileptic characteristics, such as localizing a patient's epileptogenic focus via ictal single-photon emission computed tomography (SPECT) or functional magnetic resonance imaging (fMRI) [16]. Seizure onset detection is particularly useful to neurologists who usually spend hours analyzing patients' EEG records in an attempt to locate seizure activity. In particular, they greatly reduce the volume of data that must be analyzed.

In general, there are two types of SODs, namely, patient specific and non-patient specific. In the latter, the detector is assumed to be able to detect seizures across a variety of patients, regardless of seizure type. This requires the seizure detection algorithm to learn the characteristics associated with a diverse range of epileptic seizures. This is extremely challenging simply because seizures manifest differently

in different individuals with the same type of epilepsy. For individuals who suffer from different seizure types, the way the seizure can manifest is countless. Also, certain seizures manifest differently each time within the same patient. Non-patient specific detectors are required to be extremely heterogeneous for the SOD to be of any practical use. Furthermore, the EEG signature of one patient's seizure may closely resemble the signature of abnormal, non-seizure EEG gathered from other patients. However, patient-specific SODs need only to learn the characteristics of the seizures present for a particular individual. Work in this area has shown that patient specific detectors outperform non-patient specific detectors because the detector is tailored to the EEG of that particular individual [16].

1.3.1 Challenges of Seizure Detection

There are many challenges that arise when it comes to seizure detection. One of the most challenging aspects of seizure detection is that the human brain is highly complex. The EEG signature of a particular patient's seizure may closely resemble normal EEG and vice versa. This causes the detector to miss some seizures and incorrectly detect seizures when in fact there are no seizures. The detection task is further complicated by the noisy nature of the EEG signal. Scalp EEG is highly susceptible to contamination by physiological and non-physiological sources. The sway of EEG electrode cables, the coupling of AC harmonics from electric machinery, and alterations in the electrode-skin interface can all produce non-physiological spectral changes that affect the performance of a seizure detector. Physiological artifacts, including sweat, chewing, eye-blinks, and scalp muscle contractions, also limit the performance of seizure detectors. Another property of scalp EEG that makes seizure detection challenging is the physical property of the EEG signal. Because the EEG is on the scalp, it is most sensitive to the activity of neurons on the brain surface;

therefore, the activity of neurons within deep brain structures has little to no influence on the scalp EEG. Consequently, when the epileptic neural activity evolves from brain structures deep within the brain, scalp-EEG will not pick up on the activity until it has affected neurons within the reading range of the EEG. These types of seizures are difficult to detect with high specificity and low latency.

The goal of this research is to design, implement, and evaluate a robust, real-time SOD that can efficiently detect the onset of epileptic seizures using simultaneously recorded, non-invasive EEG and ECG data.

1.4 Literature Review and Limitations

Over the past decade, extensive research has been dedicated to developing a seizure onset detector that is capable of detecting the onset of a seizure with high accuracy and low false alarm rate using a patient's EEG alone. In general, SODs generally consist of two main stages: feature extraction and classification [17] - [32]. In the feature extraction stage, relevant EEG features are extracted so as to characterize seizure and non-seizure events. In the classification stage, machine learning algorithms are trained to learn the features of each class of events so as to detect seizure from non-seizure features in new EEG.

Applying empirically determined thresholds on time-domain features is among the earliest methods for the detection of epileptic activity in long-term EEG recordings [17]. The work in [18] processes a single manually-selected channel of an ECoG recording using a maximum-likelihood classifier with Gaussian mixture model conditional densities to differentiate between a patient's normal and abnormal ECoG. The method of Hilbert marginal spectrum analysis based on Hilbert Huang transformation is employed for EEG signal processing in [19]. The detector in [20] proposes an algorithm to help detect seizures in long term iEEG based on low computational costs

methods using Spectral Power and Wavelet analysis. The detector was tested on 21 invasive iEEG records and a sensitivity of 85.39% was achieved. A wavelet decomposition technique is used in [16] to extract the energy in the lowest four frequency bands of the EEG for a patient-specific seizure onset detector using scalp-EEG. This detector presents a sensitivity of 94%, an average detection latency of 8.0 $\pm$ 3.2 seconds, and an average false alarm rate of 0.25 per hour. Instead of using wavelet decomposition to extract relevant EEG frequency bands, [21] uses an iterated filter bank in the seizure detection architecture. In [22], diffusion distances are extracted from ictal EEG as features and a Bayesian linear discriminant analyzer is employed as a classifier to detect the seizure onset in the long-term EEG of 21 patients. In [23], the fractal intercept and fluctuation index are extracted as EEG features and an extreme learning machine is employed to train a neural network classifier to detect the seizure in the EEG of 21 patients. The continuous wavelet transform is used to analyze EEG segments of patients with mesial temporal lobe epilepsy in [24], where a reference state is defined in the immediate pre-ictal data and is used to derive three features that quantify the discrimination between pre-ictal and inter-ictal states. A classifier trained on the features achieves a sensitivity of 85%. The work in [25] uses a recurrent neural network to learn and distinguish between several seizure and non-seizure features extracted directly from the EEG for a patient-specific seizure detector. A sensitivity of 56% and a false positive rate of 0.06 per hour is achieved by this model. A number of statistical features are extracted from transformed EEG signals and a least squares support vector machine (SVM) is used for classification in the seizure onset detector [26]. This model achieves an average sensitivity of 70.81%, specificity of 85.46%, and accuracy of 83.85%. In [27], a system based on spike rate measurement is proposed and evaluated for long-term iEEG. A sensitivity of 75.9% with an average false prediction rate of 0.09 per hour is achieved by this system.

In [28], the authors propose a method based on EEG signal differentiation to enhance seizure features in an attempt to better detect the onset of a seizure via a windowed variance method. A seizure is characterized by abnormal synchronization in neuron firing, and thus sharp spiking activities in quick succession are observed. It has been found that differentiation accentuates the spiking activity while suppressing the background, thus aiding in the detection of seizure onset using the windowed variance detection method. The detector in [28] achieves a sensitivity of 89.83%, latency of 9.2 seconds, and a false detection rate of 0.125 per hour. In [29], the regions of the brain involved in epilepsy are estimated by using the method of common spatial pattern (CSP) [30, 31]. The objective of this method is to extract patterns that represent the difference between one class of data and another. Thus, two corresponding periods of recordings in [29] are studied, namely, ictal epileptiform discharges (IED) and non-IED time intervals. IED time intervals are the periods including IED signals, while non-IED time intervals are the periods excluding any IED or abnormal physiological signals.

In many patients, seizures manifest in only certain EEG channels; therefore, only a limited number of electrodes are needed to capture the electric activity associated with the seizure. In many detectors, all the channels are used as inputs to the feature extraction stage. This increases the detectors complexity and introduces uninformative EEG data into the system. In an attempt to decrease the computational load of the seizure detection system and provide the detector with EEG data of epileptic origin, channel selection methods are investigated. In [32], three channel selection methods are evaluated prior to seizure detection, namely channel selection based on variance, difference in variance, and entropy. It is found that a detection system with channel selection based on variance performed similar to the situation when a neurophysiologist selects the channels containing the most relevant seizure informa-

tion. In [32], it is recommended to select the top $4-6$ channels and analyze them for seizure onset detection.

A review of interictal and ictal cardiac manifestation of epilepsy with focus on HR, HRV, and ECG changes is given in [13]. A set of time- and frequency-domain features and nonlinear parameters based on Poincare plots are extracted and analyzed from the HRV of epileptic patients [33]. The analysis concluded that ictal HRV parameters differ significantly from baseline HRV. In [12], a detector is implemented based on the features extracted in [33]. This detector achieves a sensitivity of 88.66%, specificity of 90%, and an accuracy of 88.33%. Biomedical signals are characterized by non-linear, time-varying properties making them non-stationary from a statistical point-of-view. However, the majority of analyses carried out on epileptic HRV exploit time-domain or frequency-domain methods. The recent work in [34] demonstrates that the combination of time-variant, frequency-selective, linear and nonlinear analysis approaches can be beneficially used for the analysis of HRV in epileptic patients. The work in [11] demonstrated that signal-adaptive approaches based on Matched Gabor Transform with nonlinear bispectral analysis and Empirical Mode Decomposition with time-variant nonlinear stability analysis show a noticeable difference between specific HRV ictal and non-ictal components. The general focus of the works in [11] and [34] is not to predict or detect a seizure but rather to provide additional information on the mechanisms leading to changes in the autonomic nervous system when a seizure occurs.

It is generally accepted that HRV provides additional information for the detection of seizures. Thus, the strategic combination of EEG and HRV analysis can help to develop robust seizure identification systems. The work in [35] proposes two seizure onset detectors based on the combination of newborn multi-channel EEG and HRV information. In the first detector, features extracted from EEG and HRV are

combined into a single feature vector prior to classification. This detector achieves 95.2% sensitivity and 88.6% specificity. In the second detector, EEG and HRV information are classified independently and then combined to obtain a final decision. This detector achieves 95.2% sensitivity and 94.3% specificity. A neonatal seizure detector based on the combination of simultaneously-recorded EEG and ECG is proposed in [36], where a sensitivity of 97.52% and a false alarm rate of 13.18% is obtained.

1.4.1 Limitation of Existing Methods

Several short comings are present in the existing seizure detection methods. These short comings are outlined in the following points:

- Limited research has been done in the area of EEG feature enhancement as a technique to improve seizure onset detection. Feature enhancement is a crucial component of seizure detection systems because some EEG features are more informative after certain enhancement techniques are applied. Enhancing seizure features while simultaneously attenuating non-seizure features can decrease the burden on the classification algorithm and improve the detector's overall performance in terms of sensitivity, detection onset latency, and false alarm rate. Furthermore, feature enhancement can improve the discrimination between seizure EEG and background EEG and noise.

- HRV signals are nonlinear and non-stationary in nature allowing the frequency content of the signal to vary with time. It is well documented that this variation may be crucial in the important tasks of detection [37]. However, current seizure detectors have limited their analysis of HRV to the time or frequency domains using linear and nonlinear methods. This major limitation restricts the potential of ECG and HRV signals in seizure detection, as well as decreases

the quality of features that can be extracted.

- Current state-of-the-art EEG-based, ECG-based, and EEG-ECG based seizure detectors fail to detect 100% of a patient's seizures, thus decreasing their reliability as a detection system.

1.5 Research Contributions

In an attempt to address and improve the shortcomings of current state-of-the-art SODs, we propose a novel architecture for the robust detection of epileptic seizures through the fusion of simultaneously-recorded scalp-EEG and ECG. We propose a novel detector architecture that exploits the method of CSP as a feature enhancement technique for EEG data. In the context of this thesis, feature enhancement refers to emphasizing the energy in the seizure EEG and suppressing the energy in non-seizure EEG. The proposed architecture shows that after CSP feature enhancement, seizure and non-seizure EEG are more distinct. As a result, the extracted energy features of the non-seizure EEG signal are attenuated while the energy features of the seizure EEG are amplified. Furthermore, we propose two EEG detector architectures. The first detector exploits all the features extracted from the CSP-enhanced channel-selected EEG data and feeds them into a single SVM for seizure onset detection. We refer to such a detector as a traditional-classification detector (TC-detector). In the second detector architecture, we propose a novel classification stage where each feature extracted from one of the four sub-bands is fed into a separate SVM for classification. The band-specific local classification decisions are then fused to derive a global detection decision. We refer to such a detector as band-sensitive detector (BS-detector).

In addition, because time-frequency (TF) representations are able to localize the signals energy in both time and frequency by mapping a one-dimensional sig-

nal into a two-dimensional representation, we adopt a signal adaptive, quadratic time-frequency distribution approach in analyzing HRV based on the combination of the Matching-Pursuit (MP) and Wigner-Ville Distribution (WVD) algorithm. This method enables the extraction of more meaningful features from HRV data, and thus, it improves the classification and detection stages.

The features extracted from the EEG and ECG signals are independently classified and then their independent decisions are fused to output a single decision. Our experimental results indicate that such a fused system can lead to an improved detection performance in terms of accuracy, false alarm rate, and latency compared with other state-of-the-art detectors. Specifically, the contributions of this work can be summarized as follows:

- A SOD is developed based on the fusion of EEG and ECG data. The detector consists of an EEG-based detection system, an ECG-based detection system, and a fusion system.

- In the EEG-based detection system, a CSP-based feature enhancement stage is implemented on scalp-EEG to emphasize the seizure features while attenuating the non-seizure features. The features are extracted from four seizure-relevant frequency bands, which are then classified independently and then fused according to different fusion methods.

- In the ECG-based detection system, a combined MP-WVD algorithm is applied to HRV data prior to feature extraction so that more meaningful features can be analyzed compared with features extracted only from the time- or frequency-domain.

- Two EEG/ECG fusion systems are investigated, namely, the direct fusion sys-

tem and over-ride fusion system.

- The performance of the proposed fusion detector is evaluated and compared with the state-of-the-art detectors. The proposed detectors achieve 100% sensitivity and specificity of over 99%.

1.6 Overview of Thesis

The remainder of the thesis is organized as follows. Chapter 2 describes the components making up the EEG-based SOD. Chapter 3 evaluates the performance of the EEG-based SOD on a set of clinical patients and compares the results with state-of-the-art SODs. Chapter 4 discusses and evaluates the ECG-detection unit. In Chapter 5 the EEG-ECG fusion SOD is presented and its performance is evaluated and compared to state-of-the-art detectors. A preliminary investigation regarding the use of neural synchrony as a seizure detection measure is presented in Chapter 6. Finally, concluding remarks are given in Chapter 7.

2. EEG-BASED SEIZURE ONSET DETECTION*

In this chapter, two novel epileptic SODs are proposed. The detectors rely on a CSP based feature enhancement stage that increases the variance between seizure and non-seizure scalp EEG. The proposed feature enhancement stage enables better discrimination between seizure and non-seizure features. The first detector adopts a conventional classification stage using a SVM that feeds the energy features extracted from different sub-bands to a SVM for seizure onset detection. The second detector uses logical operators to pool SVM seizure onset detections carried out independently across different EEG spectral bands.

2.1 Introduction

The proposed seizure detection algorithm adopts the concept of binary classification for seizure detection. Binary classification is the process of assigning an observation to one of two classes. In the problem at hand, an EEG segment must be classified as either pertaining to the seizure class or non-seizure class of EEG. Determining the class membership of an observation involves two basic steps. First, salient features that efficiently discriminate between the two classes are extracted from the observation (EEG segment). In the case of seizure detection in EEG data, energy is an excellent feature that effectively distinguishes between seizure and non-seizure EEG. Secondly, a classifier must be trained to recognize the difference between the features of each class so that it can accurately determine the class membership of new, unlabeled data (observation) based on its extracted features.

The success of a binary classification task strongly depends on the features ex-

* Part of this chapter is reprinted with permission from "Band-sensitive seizure onset detection via CSP-enhanced EEG features" by Marwa Qaraqe, Muhammad Ismail, and Erchin Serpedin, 2015, *Epilepsy and Behavior*, vol. 50, pp. 77-87.

tracted from the data and the type of classification algorithm employed to determine class membership. Ideally, the best features are those that have a distribution of values for one class that are very different than the distribution of values for the second class. Therefore, a major factor that affects the performance of SODs is the quality of features extracted from the EEG. In the proposed SOD, a CSP based feature enhancement stage is implemented in order to maximally differentiate between seizure and non-seizure features.

Another factor that contributes to the success of detection algorithms is the amount of pertinent information available versus the amount of invaluable information contained in the data. To address this issue, a channel selection unit has been implemented in the proposed detection algorithm.

2.2 Feature Processing Stage

This section presents the EEG feature processing stage of the proposed detectors. Such a stage is composed of three units, namely, channel selection, feature enhancement, and feature extraction, as shown in Figure 2.1.

2.2.1 Channel Selection

The aim of the channel selection stage is to automatically choose the EEG channels that contain the most valuable electrographic seizure information. This in turn reduces the detector's computational burden and omits information from invaluable channels that may deteriorate the detector's performance.

The channel selection method used in this work is based on the amount of variance in the seizure EEG signal amplitude. The rationale is that during a seizure episode, higher signal energy is observed as compared with the non-seizure case, and this energy can be measured through variance. The variance in the seizure period of

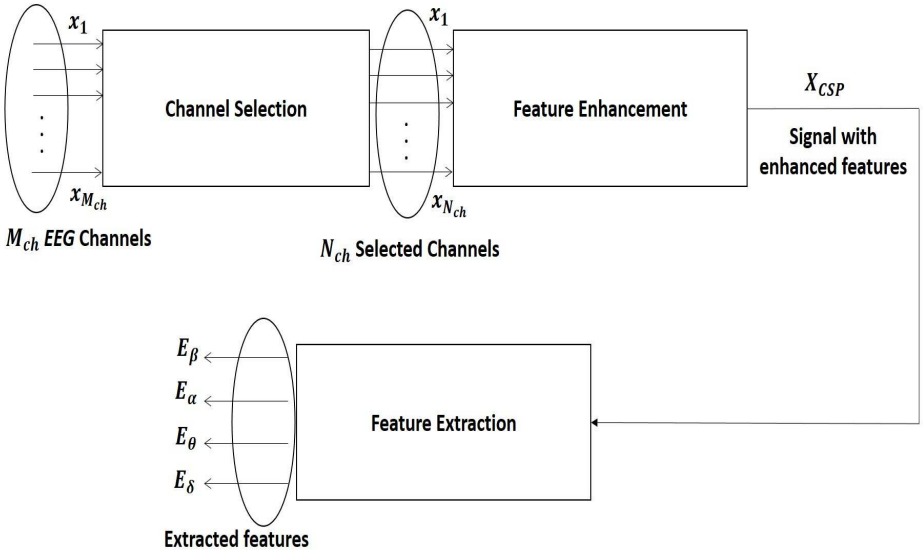

Figure 2.1: EEG Feature Processing Stage.

channel c, $V_s(c)$, is expressed by,

$$V_s(c) = \frac{1}{I}\sum_{i=1}^{I}(x_c(i) - \mu_c)^2 \tag{2.1}$$

where x_c is the seizure EEG data for channel c, μ_c is the mean of the seizure EEG data for channel c, and I is the number of samples in the seizure EEG data (equal to the sampling frequency multiplied by the duration, in seconds, of the seizure EEG). Let $\mathcal{M}_{ch}$ and $\mathcal{N}_{ch}$ denote the set of available and selected EEG channels, respectively. The $\mathcal{N}_{ch}$ selected channels are chosen as the ones with the highest variance values, and are given by

$$\mathcal{N}_{ch} = \arg\max V_s(c), \tag{2.2}$$

where $c \in \mathcal{M}_{ch}$ and $N_{ch} < M_{ch}$ is defined as the number of selected channels. Thus, assuming the EEG record of interest contains I sample points, the new EEG matrix after channel selection will have size $N_{ch} \times I$. In this work, we select the highest 5

channels (i.e., $N_{ch} = 5$).

The channel selection is done offline using a single EEG recording of a particular patient. Once the N_{ch} channels have been identified, these channels are then automatically chosen in all future online EEG recordings for that particular patient.

2.2.2 CSP-based Feature Enhancement

CSP is a method that uses a linear transform to project multi-channel EEG data onto a low-dimensional spatial subspace with a projection matrix, Z, of which each row consists of weights for each of the channels. In order to discriminate between the two classes of EEG signals, seizure and non-seizure, the spatial filters are designed so that each can extract temporal sequences of maximum variance from one class of EEG signals (which corresponds to the minimum variance for a second class of EEG signals). This is achieved by the simultaneous diagonalization of the covariance matrices of both classes of EEG signals. In essence, the main idea of CSP filtering is to maximize the difference in variance between two classes of EEG signals. When this is done, more discriminatory features between the two EEG classes can be extracted. The mathematical details are outlined below [30].

Let X be an EEG matrix of size $N_{ch} \times E_c$ containing a single seizure episode, where N_{ch} denotes the number of EEG channels and E_c represents the number of digital samples taken from each channel. Assume the seizure starts at time t_1 and ends at t_2 for a total duration of T_s-seconds. Let X_s be a $N_{ch} \times T_s$ matrix that corresponds to the seizure EEG data extracted from X. Similarly, let X_{ns} be a $N_{ch} \times T_s$ matrix that corresponds to the non-seizure EEG data extracted from X for a duration of T_s seconds of non-seizure EEG. The normalized spatial covariance

matrices of X_s and X_{ns} are represented as

$$R_s = \frac{X_s X_s^{'}}{\text{trace}\,(X_s X_s^{'})} \tag{2.3}$$

and

$$R_{ns} = \frac{X_{ns} X_{ns}^{'}}{\text{trace}\,(X_{ns} X_{ns}^{'})} \tag{2.4}$$

respectively, where $X^{'}$ is the transpose of X and trace(A) computes the sum of the diagonal elements of matrix A. The composite normalized covariance matrix is given by

$$R_c = R_s + R_{ns}. \tag{2.5}$$

This composite covariance matrix is then factored into products of three matrices using the method of eigenvalue decomposition as follows

$$R_c = U \Lambda U^{'}, \tag{2.6}$$

where U is the $N_{ch} \times N_{ch}$ matrix of eigenvectors and Λ is the $N_{ch} \times N_{ch}$ diagonal matrix of eigenvalues. A whitening transformation matrix, P, can be formed as follows:

$$P = \frac{U^{'}}{\sqrt{\Lambda}}. \tag{2.7}$$

It can be shown that if R_s and R_{ns} are individually transformed such that

$$S_s = P R_s P^{'} \quad \text{and} \quad S_{ns} = P R_{ns} P^{'}, \tag{2.8}$$

then S_s and S_{ns} share common eigenvectors (basic spatial patterns) and the sum of the corresponding eigenvalues for the two matrices will always be 1. In particular, if

S_s is factored such that

$$S_s = V D_s V^{'} \tag{2.9}$$

and S_{ns} is factored such that

$$S_{ns} = V D_{ns} V^{'}, \tag{2.10}$$

then

$$D_s + D_{ns} = I, \tag{2.11}$$

where I represents the identity matrix, D_s denotes the diagonal eigenvalue matrix corresponding to S_s, D_{ns} stands for the diagonal eigenvalue matrix corresponding to S_{ns}, and V is the common eigenvector matrix of both S_s and S_{ns}.

This result is extremely valuable for the separation of two classes of EEGs, seizure and non-seizure EEG, since the eigenvectors will be in the subspace that maximizes the number of the components belonging to that subspace. More specifically, with respect to the whitened measurement space spanned by V, if the eigenvalues of S_s and the corresponding eigenvectors are arranged in descending order, then the variance accounted for by the first m-eigenvectors will be maximal for X_s, where $m \in [1, \frac{N_{ch}}{2}]$ and $\frac{N_{ch}}{2}$ is an integer. In the event that N_{ch} is odd, $\frac{N_{ch}}{2}$ is rounded to the nearest integer. Because of the sum constraint in (2.11), the variance accounted for by these m-eigenvectors must be minimal for X_{ns}. In other terms, the eigenvectors with the largest eigenvalues for S_s will have the smallest eigenvalues for S_{ns}, and vice versa.

The eigenvalue matrix can be expressed as

$$V = [\mathbf{v_1 v_2} \cdots \mathbf{v_{N_{ch}}}], \tag{2.12}$$

where $\mathbf{v_i}$ is a column vector that corresponds to the i^{th} eigenvector of V. The eigenvalues of S_s and its corresponding eigenvectors are arranged in a descending

order so that the first column of V corresponds to the vector that accounts for the maximum variance for X_s and minimum variance for X_{ns}. For maximal seizure enhancement, only vector $\mathbf{v_1}$ is chosen from V so that

$$\mathbf{z} = \mathbf{v_1}^{'} P = [z_1 \ z_2 \ \cdots \ z_{N_{ch}}] \tag{2.13}$$

is a projection vector of size $1 \times N_{ch}$. The projected vector contains the optimal set of weights that maximize the variance of seizure events and simultaneously minimize the variance of non-seizure events. The components of the projection vector, $\mathbf{z}$, are the spatial filters that yield non-uniform weights to EEG channels so that the difference between the two classes of EEG signals (i.e., seizure and non-seizure) is maximized in terms of variance.

For a particular patient, the projection vector, $\mathbf{z}$, is extracted offline from a single EEG recording of that patient (X). Once $\mathbf{z}$ has been a identified, all future EEG data can be enhanced (online) by

$$Q_{CSP} = \mathbf{z}Q \tag{2.14}$$

where Q is an EEG data matrix independent of X and Q_{CSP} is the CSP version of the original EEG matrix Q.

2.2.3 Feature Extraction

This section discusses the feature extraction methodology adopted in the EEG-based SOD. The extraction of salient features from the input data is a crucial step in any application of seizure detection. In this work, salient features are extracted from the EEG signal after it has gone through the feature enhancement unit. Features are usually extracted from reasonably small time segments (epochs) due to the highly

non-stationary characteristics of EEG signals. A sliding window of length $L = 2$ seconds is moved along the EEG signal by one-second intervals in order to extract the 2-second epoch. Each epoch is then fed into the feature extraction unit.

2.2.3.1 Wavelet Transform

The onset of a seizure is often associated with rhythmic activity that is composed of multiple frequency components. In order to detect seizures with high accuracy, it is important to consider the multiple spectral components that relate to epileptic activity. Therefore, in an attempt to improve detection accuracy, features should be extracted from several EEG sub-bands. The EEG activity of clinical relevance is limited to the frequency band $0.5 - 50$ Hz; however, the frequency range that captures various seizure onset electrographic manifestations is $0.5 - 25$ Hz. The sub-band signals that collectively represent the activity at time-scales corresponding to the seizure frequencies are the δ, θ, α, and β EEG frequency bands, where $\delta < 4$ Hz, $\theta \in [4, 7]$ Hz, $\alpha \in [8, 15]$ Hz, and $\beta \in [16, 31]$ Hz.

In order to extract relevant sub-band signals from a given EEG epoch, a multi-resolution wavelet decomposition is used. In a multi-resolution wavelet decomposition, the signal of interest is passed through an iterated filter bank, similar to that in Figure 2.2, to extract sub-band signals of interest. The time scale or frequency of activity resolved by a particular sub-band signal is determined by the iteration level producing it and the choice of the analysis filters $H_0(z)$ and $H_1(z)$. The low and high pass filters, $H_0(z)$ and $H_1(z)$, are chosen to be associated with the fourth member of the Daubechies wavelet family as these filters exhibit a maximally flat response in their passband as well as little spectral leakage in their stop bands [38].

Generally, the sub-band signals produced by higher iteration levels contain lower frequency components and capture long time-scale activity, while those produced

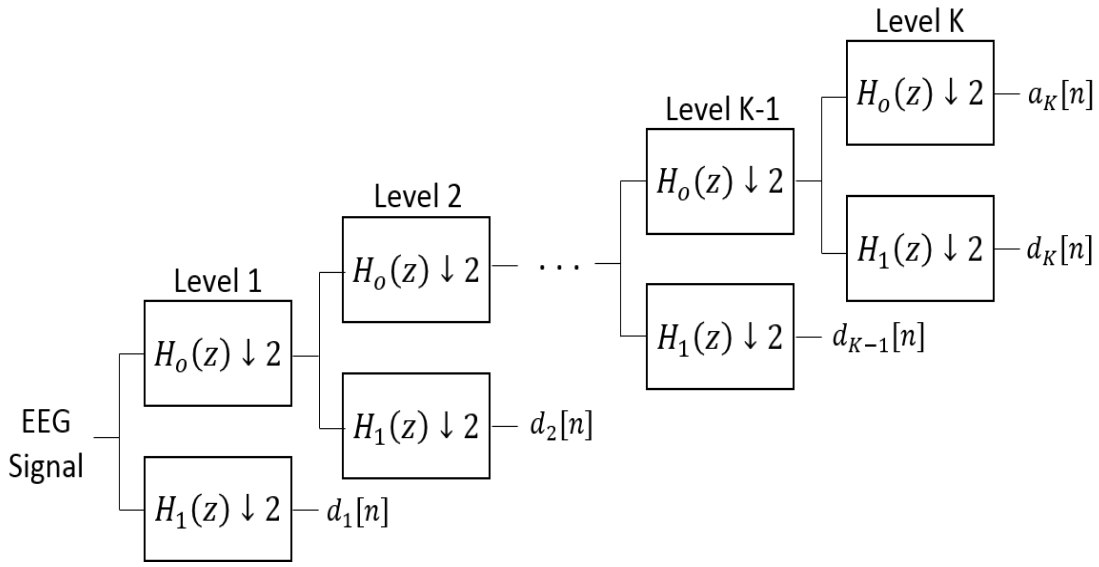

Figure 2.2: Multilevel wavelet decomposition filter bank. The choice of the analysis filters, $H_1(z)$ and $H_0(z)$, determines the time scale of activity captured within each sub-band signal [16].

by lower iteration levels contain higher frequency components and capture shorter time-scale activity. For the purpose of seizure detection, only sub-band signals $\{d_4[n],\ d_5[n],\ d_6[n],\ d_7[n]\}$ are computed because collectively they represent the activity at time scales corresponding to frequencies from 0.5 to 25 Hz. In particular, the sub-band signals $d_4[n], d_5[n], d_6[n]$, and $d_7[n]$ correspond to the β, α, θ, and δ bands, respectively. This is evident from the frequency response of the cascaded filters shown in Figure 2.3. The lowest level sub-band signal is associated with the widest bandwidth frequency response, while the highest level sub-band signal is associated with the narrowest bandwidth frequency response. The impulse responses of the cascaded filters are shown in Figure 2.4 for levels 4, 5, 6, and 7. The lowest level sub-band signals are associated with the shortest time-scale impulse response, while the highest level sub-band signal is associated with the largest time-scale impulse response.

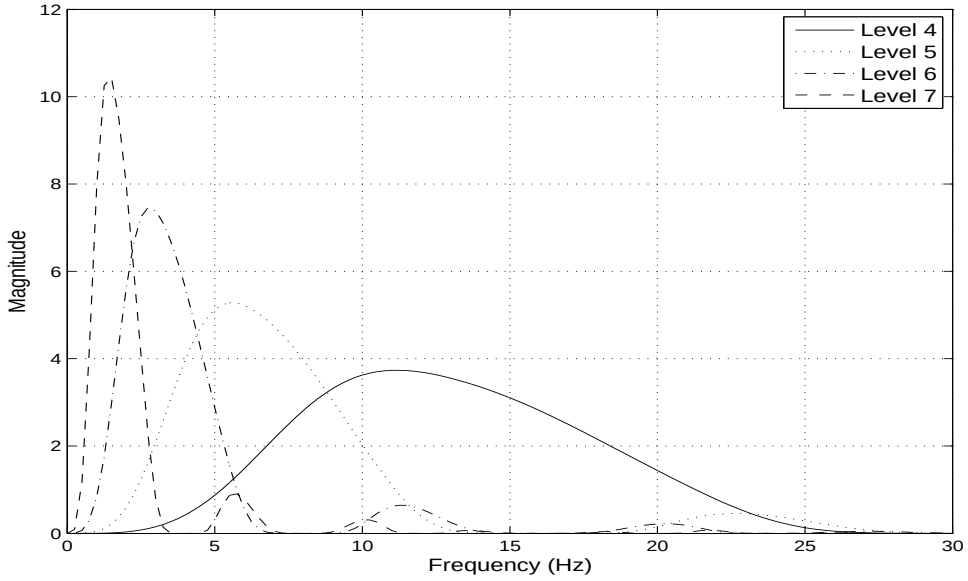

Figure 2.3: Frequency response of the wavelet filter bank for levels 4, 5, 6, and 7. Lowest level sub-band signal is associated with the widest bandwidth frequency response. Highest level sub-band signal is associated with the narrowest bandwidth frequency response.

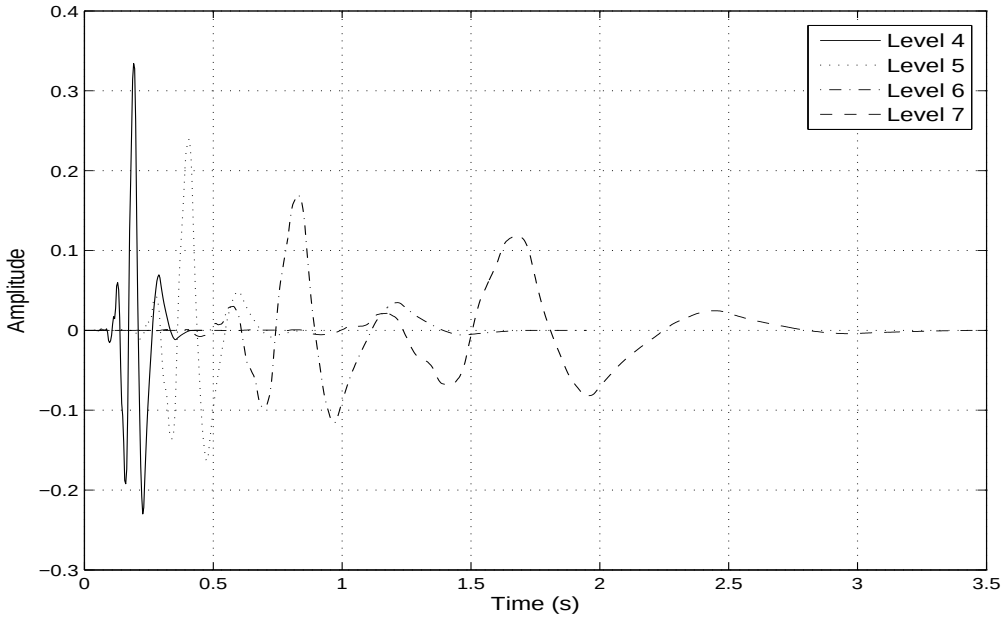

Figure 2.4: Impulse response of the wavelet filter bank for levels 4, 5, 6, and 7. Lowest level sub-band signals are associated with the shortest time-scale impulse response. Highest level sub-band signal is associated with the largest time-scale impulse response.

The remaining sub-band signals primarily resolve activity of no clinical relevance with respect to seizure onset detection. For example, the sub-band signal $a_7[n]$ captures slow baseline variations (i.e., caused by sweating). The sub-band signals $\{d_1[n],\ d_2[n],\ d_3[n]\}$ capture high-frequency components that usually signify artifacts similar to those resulting from muscular contractions.

2.2.3.2 Energy Feature Extraction

The extracted sub-band signals are not used directly as feature vectors since direct representation of the EEG waveform is too sensitive to noise. Instead, the energies contained in the four sub-bands are computed as features. Exploiting the energy information of a signal that has been enhanced via CSP provides the most relevant information in discriminating between two classes. In particular, once CSP is applied to an EEG signal, the amplitudes of the signals change such that they have an increased difference for seizure and non-seizure signals. Consequently, the feature that can best quantify the difference between the amplitudes is energy.

The energies in the two-second epoch sub-bands are computed as follows

$$\begin{bmatrix} E_\beta \\ E_\alpha \\ E_\theta \\ E_\delta \end{bmatrix} = \begin{bmatrix} \sum(G_\beta^2) \\ \sum(G_\alpha^2) \\ \sum(G_\theta^2) \\ \sum(G_\delta^2) \end{bmatrix}, \tag{2.15}$$

where G_β, G_α, G_θ, and G_δ are the sub-band signals extracted from a particular epoch, the summation is taken over the sample points in the epoch, and E_β, E_α, E_θ, and E_δ are the energies in the β, α, θ, and δ sub-bands of the epoch, respectively.

2.3 Classification Methodology

In this section, the classification stages of the two proposed detectors are discussed. The first detector classification stage provides the SVM with all features extracted from the four sub-bands in a single feature vector. The second detector classification stage is composed of two units. The first unit finds the detection decisions for each sub-band independently of the other sub-bands. Hence, the energy feature extracted from each sub-band is fed into an SVM. The second unit fuses the band-specific decisions to derive the global detector decision. The rationale behind such a classification methodology will be explained later.

In an attempt to decrease the number of false seizure detections, a timing constraint, T_c, is adopted in both detectors. The timing constraint does not allow the detector to declare a seizure event until SVM has detected T_c consecutive seizure epochs. Using a large value for T_c will decrease the detectors false alarm rate; however, it will increase the time between the actual seizure onset and the time when the detector raises an alarm. Small values for T_c will decrease the time difference between an actual seizure onset and the detector-based onset, but will increase the false alarm rate of the detector. In this work, we adopt $T_c = 3$. Therefore, the detectors must observe at least 6 seconds of seizure activity in the EEG before declaring a seizure event.

2.3.1 SVM

In the proposed detectors, an SVM-based classifier is used to classify a new feature vector as either belonging to a seizure brain state or a non-seizure brain state. SVMs must be trained on feature vectors representing both seizure and non-seizure EEGs. After training, SVMs are able to determine the class membership of a newly observed feature vector based on which side of a separating hyperplane the observation lies.

Hence, for each patient, the SVM is trained offline on an EEG record of that patient. Following such a training, the SVM is able to detect a seizure event online from a new EEG record.

The hyperplane separating the two classes is defined to be maximally distant from the boundary cases of each class. The boundary cases are defined as support vectors carrying the information relevant to solving the classification problem. In the case of seizure detection, a linear hyperplane cannot accurately separate seizure features from non-seizure features; therefore, SVMs generally use more complex, non-linear kernels to determine the decision boundary (separating hyperplane). The SVM software used for classification purposes in this work is based on the built-in SVM algorithm in the MatLab software and the Gaussian radial basis function (RBF) is chosen as the non-linear kernel.

The ability of an SVM to discriminate between two classes is influenced by several factors, namely, their separability, the parameters of the chosen kernel, and the class-specific penalty for determining a decision boundary that misclassifies a percentage of training samples, C. The RBF's sole parameter, σ, influences the sophistication of the decision boundary. Small values of σ will translate into an increasingly sophisticated boundary that correctly classifies a higher percentage of training examples. In addition, large values for C favors the determination of a decision boundary that correctly classifies the training examples. Therefore, extreme choices for both of these variables increase the risk of over-fitting the data, causing SVM to perform poorly on a new set of data. As a result, in this work, σ is set to 1 and equal class-specific penalties for seizure and non-seizure classes is chosen ($C = 1$).

2.3.2 Traditional Classification

In the traditional classification (TC) detector, each EEG epoch is assigned to a seizure or non-seizure class using an SVM that is trained on feature vectors representing both seizure and non-seizure epochs. The feature vector fed into the SVM is composed of the energy contained in each frequency sub-band of the EEG epoch, as given in (2.15). Therefore, the SVM uses all the information from all extracted features simultaneously to classify an EEG epoch. Figure 2.5 shows a block diagram illustrating the detector's architecture. The feature processing block includes all components shown in Figure 1.

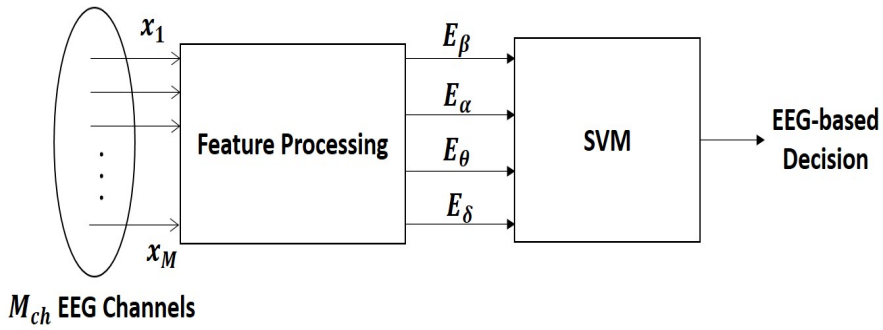

Figure 2.5: An illustration of TC-detector architecture. The feature processing block includes all components shown in Figure 2.1.

2.3.3 Band-Sensitive Classification

A novel classification stage is proposed based on the fusion of band-specific local decisions, as shown in Figure 2.6. The classification stage is based on two major units. In the first unit, the energy contained in the four frequency sub-bands are separately classified by different SVMs that have been trained offline by features from the respective energy band. The decision of each SVM, ($D_\beta, D_\alpha, D_\theta$, and D_δ)

will classify the features from each sub-band as either belonging to the seizure class, denoted by 1, or the non-seizure class, denoted by 0. The second unit of the classification stage is a fusion unit that combines the output of all four SVMs to yield a single global decision.

The motivation behind adopting such a detector is to investigate the electrographic manifestation of epileptic seizures in the β, α, θ and δ frequency bands. Certain seizures portray unique electrographic alterations in specific frequencies. Therefore, analyzing each frequency sub-band separately allows for the deep investigation of such manifestations. Additionally, for some patients, specific bands exhibit maximum separation between seizure and non-seizure events using the CSP-based feature enhancement stage. Investigating separate frequency bands enables an improved detection performance, as will be shown in Chapter 3.

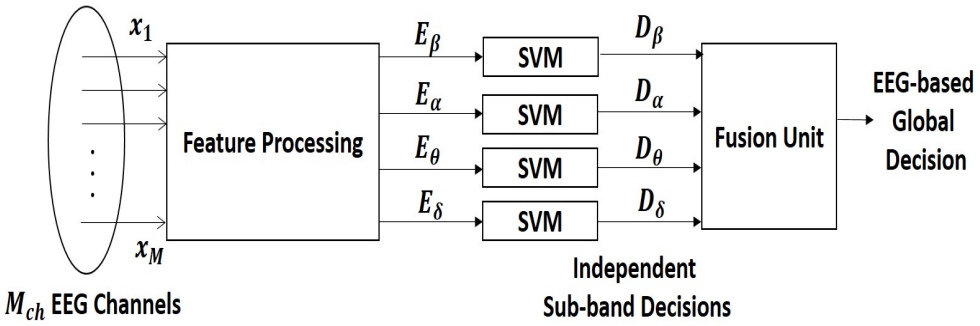

Figure 2.6: An illustration of the BS-architecture. The feature processing block includes all components shown in Figure 2.1.

Three different fusion techniques are analyzed in the BS-detector, as outlined below.

2.3.3.1 AND Fusion

The first fusion technique is based on the AND logical operator, where all four sub-band signals must be classified as seizure for the global decision to yield a seizure result. Otherwise, the global result will be non-seizure. This can be expressed by

$$D_\beta \wedge D_\alpha \wedge D_\theta \wedge D_\delta = 1, \tag{2.16}$$

if and only if $D_\beta = D_\alpha = D_\theta = D_\delta = 1$ and

$$D_\beta \wedge D_\alpha \wedge D_\theta \wedge D_\delta = 0, \tag{2.17}$$

otherwise, where $\wedge$ denotes the AND logical operator.

2.3.3.2 OR Fusion

The second fusion technique is based on the OR logical operator. Here, the global decision can declare a seizure event if at least one of the sub-band decisions yields a seizure event. This is described by

$$D_\beta \vee D_\alpha \vee D_\theta \vee D_\delta = 0, \tag{2.18}$$

if and only if $D_\beta = D_\alpha = D_\theta = D_\delta = 0$ and

$$D_\beta \vee D_\alpha \vee D_\theta \vee D_\delta = 1, \tag{2.19}$$

otherwise, where $\vee$ denotes the OR logical operator.

2.3.3.3 MAJORITY Fusion

In the third fusion technique, the global decision can only declare a seizure event if and only if more than 50% of the sub-band decisions are seizure events. This fusion technique is the majority (MAJ) method. The MAJ operator can be expressed as

$$MAJ = B_1 \vee B_2 \vee B_3 \vee B_4 \tag{2.20}$$

where $B_1 = D_\beta \wedge D_\alpha \wedge D_\theta$, $B_2 = D_\beta \wedge D_\alpha \wedge D_\delta$, $B_3 = D_\alpha \wedge D_\theta \wedge D_\delta$, and $B_4 = D_\beta \wedge D_\theta \wedge D_\delta$. For $MAJ = 1$, either B_1, B_2, B_3, or B_4 should yield 1, and in order for B_1, B_2, B_3, or B_4 to yield 1, all of their sub-components must be 1. Therefore, the MAJ operator guarantees that for a seizure to be declared as a global decision, at least three of the four sub-bands must have been classified as seizure events.

3. EEG-BASED SOD PERFORMANCE RESULTS*

This chapter analyzes the effectiveness of the proposed feature enhancement unit and BS-classification method of the EEG-based SOD introduced in Chapter 2. The performance results for the EEG-based SOD on a set of clinical patients are also evaluated and compared to the state-of-the-art SODs.

3.1 Clinical Data

The data used to evaluate the proposed detectors in this chapter is from a publicly available database consisting of EEG recordings from pediatric subjects with intractable seizures, collected at the Children's Hospital Boston (CHB) [39]. The subjects have been monitored for up to several days following withdrawal of anti-seizure medication in order to characterize their seizures and assess their candidacy for surgical intervention. The CHB database includes 23 patients where each patient has between 9 to 42 continuous EEG recordings and exhibits between 3 to 14 seizures. All signals are sampled at 256 samples per second with 16-bit resolution. The International $10-20$ System of EEG electrode positions and nomenclature is used for these recordings. All recordings have 23 EEG channels.

For each clinical seizure, an expert has indicated the earliest EEG change associated with the seizure. The data is segmented into one hour long records. Records that do not contain a seizure are referred to as non-seizure records and those that contain one or more seizures are referred to as seizure records. Furthermore, the recordings are made in a routine clinical environment, so non-seizure activity and artifacts such as head/body movement, chewing, blinking, early stages of sleep, and

*Part of this chapter is reprinted with permission from "Band-sensitive seizure onset detection via CSP-enhanced EEG features" by Marwa Qaraqe, Muhammad Ismail, and Erchin Serpedin, 2015, *Epilepsy and Behavior*, vol. 50, pp. 77-87.

electrode pops/movement are present. No constraints regarding the types of seizure are imposed; the data set contains focal, lateral, and generalized seizures.

No form of pre-processing for artifact and noise removal has been performed on the data. Our approach to deal with artifacts is based on training our detector to recognize artifacts rather than actively removing them using standard signal processing techniques.

3.2 Effectiveness of the EEG Feature Enhancement Unit

In this section, the effect of applying CSP on EEG signals that contain seizure events is analyzed. The CSP projection vector consists of spatial weights that are optimized to maximize the variance between two classes, i.e., seizure and non-seizure EEG. For comparison purposes, an equal-weight spatial averaging (EWSA) method has also been adopted. Such a benchmark resembles existing detector architectures that do not include a feature enhancement stage. In the EWSA, the N_{ch} channels of an EEG matrix Q are averaged with equal weights so that a single EEG vector, $\mathbf{q}$, is obtained. More specifically, let $\mathbf{b}$ be the equal weight vector

$$\mathbf{b} = \left[\frac{1}{N_{ch}} \ \frac{1}{N_{ch}} \ \cdots \ \frac{1}{N_{ch}} \right]. \tag{3.1}$$

Therefore, each EEG channel has an equal averaging coefficient of $\frac{1}{N_{ch}}$, and the output vector of EWSA is given by $\mathbf{q}_{EWSA} = \mathbf{b}Q$.

3.2.1 CSP Enhanced EEG

Figures 3.1 and 3.2 depict a one-hour long EEG record of patient 1 under EWSA and CSP, respectively. The blue signals correspond to the non-seizure EEG data and the red signals represent seizure EEG data. The start and end of the seizure is from 1015 seconds till 1066 seconds. The seizure part of the EEG record under

EWSA cannot be easily detected from the background EEG (non-seizure EEG). Specifically, the EEG waveforms from 2350 to 3500 seconds closely resemble the seizure EEG under EWSA. This similarity between seizure and non-seizure EEG makes it difficult to extract features that uniquely differentiate seizure events from non-seizure events, leading to poor performance of the detector. However, after CSP filtering, the seizure EEG amplitude is measured between -140 μ-volts to 140 μ-volts, while that of the non-seizure is measured between -30 and 30 μ-volts, on average. The advantage of CSP filtering is immediately made clear in Figure 3.2.

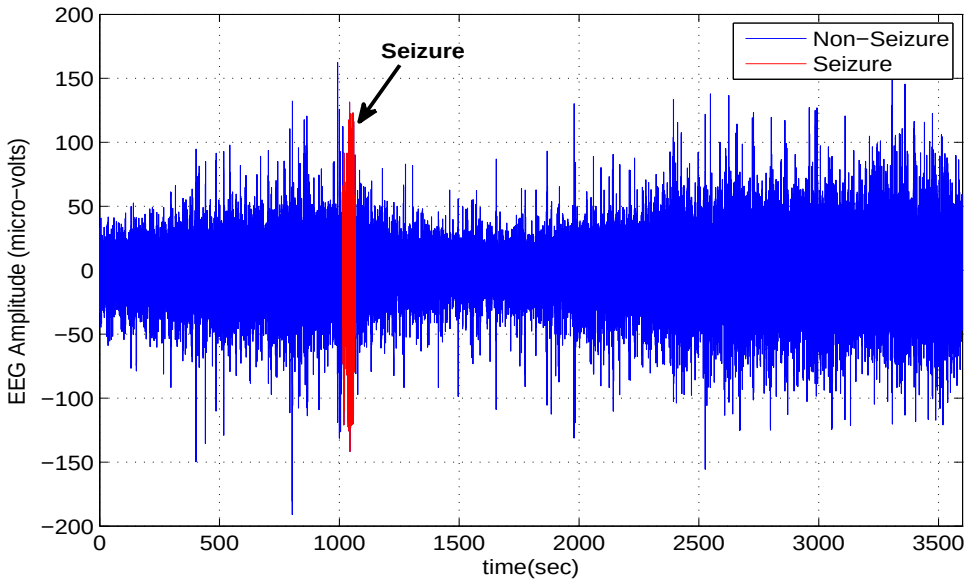

Figure 3.1: EEG record of patient 1 using EWSA. Seizure is shown in red and marked by the arrow. Blue indicates non-seizure activity.

Figure 3.3 depicts a one-hour long EEG record of patient 3 where all the channels of the record undergo EWSA. The start and end of the seizure are highlighted in red, starting from 2162 seconds till 2214 seconds. The non-seizure EEG here is also depicted in blue. The seizure part of the EEG record cannot be easily recognized as it

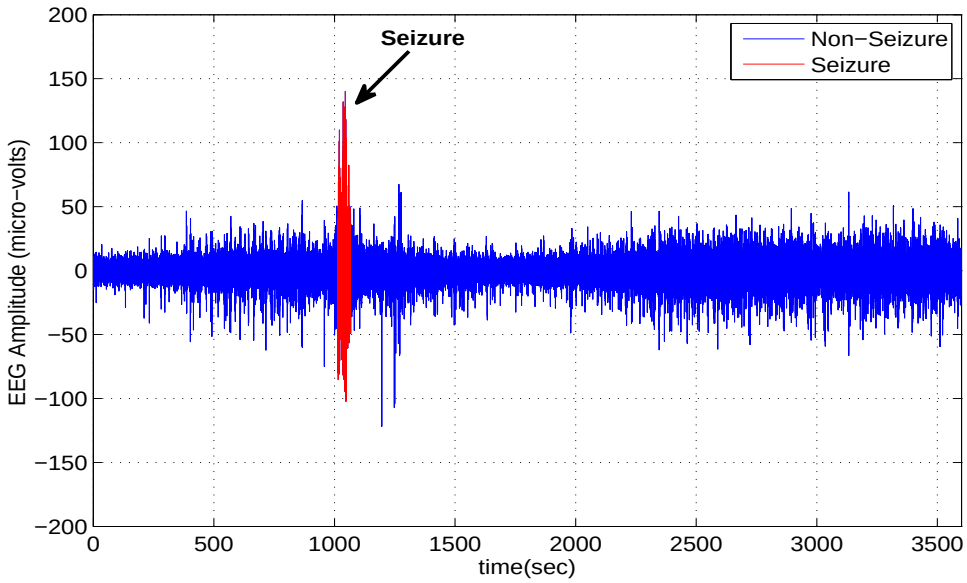

Figure 3.2: EEG record of patient 1 using CSP. Seizure is shown in red and marked by the arrow. Blue indicates non-seizure activity.

blends in with the non-seizure EEG. Furthermore, EEG waveforms at 700 seconds, 1200 seconds, 1650 seconds, and from 1900 to 2400 seconds closely resemble the seizure EEG. The similarity between seizure and non-seizure EEG creates a difficulty in extracting features that uniquely represent seizure events from non-seizure events, thus causing the detector to perform poorly.

Figure 3.4 illustrates the EEG record of patient 3 after CSP feature enhancement. Once again, the effect of CSP on separating seizure and non-seizure EEG is evident. The seizure EEG amplitude, shown in red, is measured between -400 μ-volts to 400 μ-volts, while that of the non-seizure is measured between -70 and 70 μ-volts, on average. It is clear that CSP filtering significantly increases the difference between the seizure and non-seizure amplitudes so that seizure instants are more prominent and do not resemble non-seizure data.

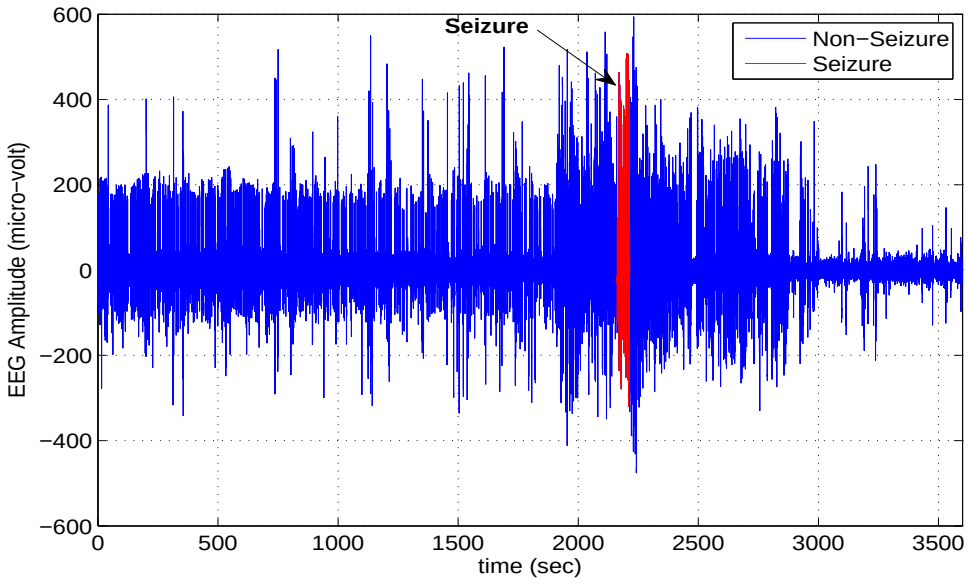

Figure 3.3: EEG record of patient 3 after EWSA. Seizure is shown in red and marked by the arrow. Blue indicates non-seizure activity.

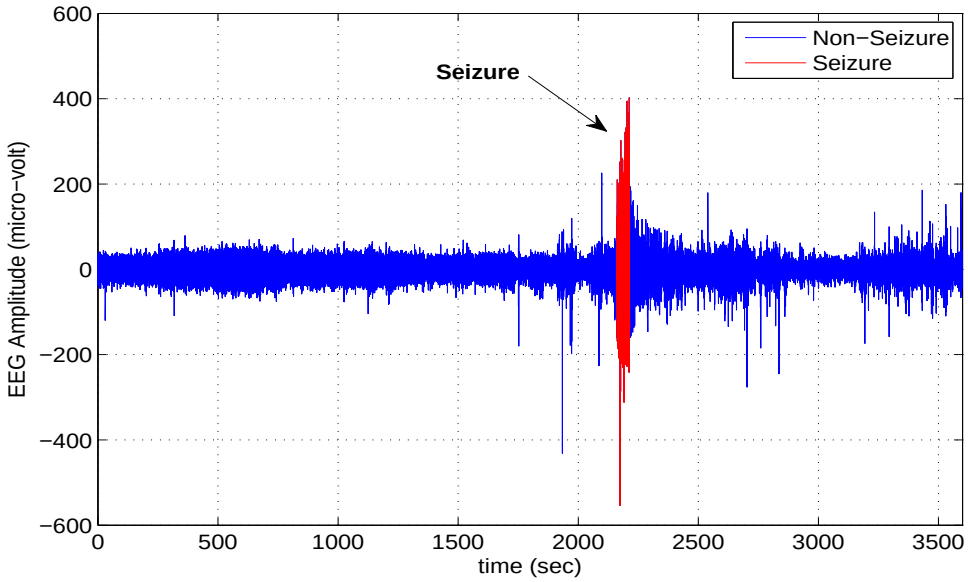

Figure 3.4: EEG record of patient 3 after CSP. Seizure is shown in red and marked by the arrow. Blue indicates non-seizure activity.

3.2.2 CSP Enhanced EEG Features

The effectiveness of a detector to discriminate between seizure and non-seizure epochs depends greatly on the quantitative difference between the extracted seizure and non-seizure features. The more discriminatory the seizure and non-seizure features are from each other, the better the classification stage performs. Figures 3.5-3.8 illustrate the difference in energy between the pre-seizure state and seizure state for all four frequency sub-bands under the EWSA and CSP scenario for seven epileptic patients. The pre-seizure duration is measured before the seizure event by approximately 90 seconds.

The energy difference for CSP feature enhancement is greater than EWSA for all patients and all sub-bands, except for the β-band of patient 2. The information contained in the β-frequency band for the second patient might not be relevant to the manifestation of the seizure and can pertain to other non-seizure related events. As a result, CSP will not enhance irrelevant, non-seizure information. In general, some frequency bands will contain more seizure-related information than others, and CSP puts emphasis only on seizure-related events, causing energy difference in some bands to be enhanced more than others in terms of seizure features. This phenomenon motivates building a band-sensitive detector that strategically exploits the information within the bands that contain significant seizure information, instead of using all bands regardless of whether they contain useful information. This, as will be seen in the next section, will increase the detector's performance. The benefit of increased energy difference between pre-seizure and seizure epochs is observed in the detection latency, the time between the expert marked seizure onset and the detector's alarm, and the ability of the detector to correctly recognize the onset of a seizure. If the pre-seizure and seizure energies are similar, the classifier will take

longer to identify seizure epochs, whereas if there is a distinct difference between the two periods, the seizure onset can be identified earlier and more accurately.

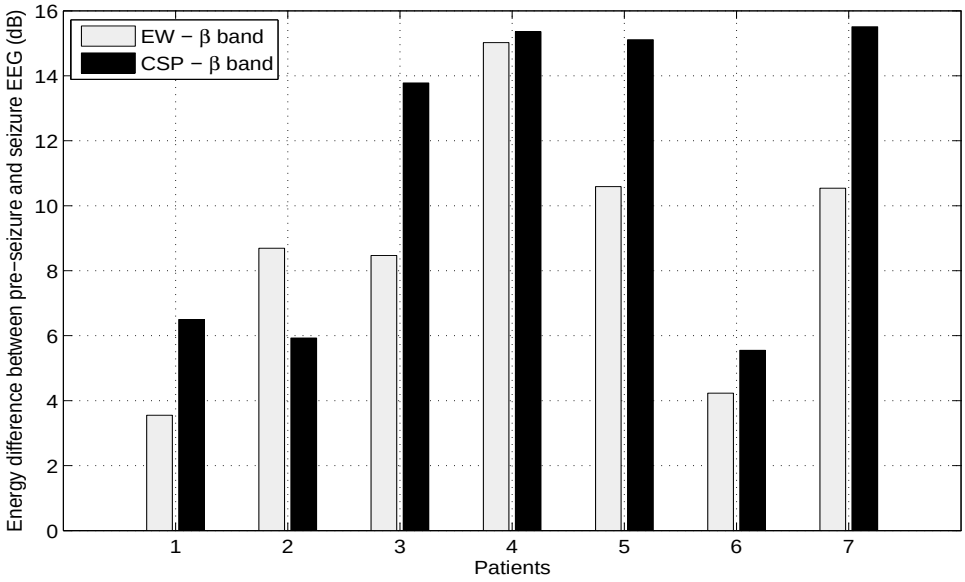

Figure 3.5: Average difference in energy between the pre-seizure and seizure EEG in the β frequency sub-band.

Figure 3.9 shows the energy in the β-frequency band when feature extraction is done on the EEG waveform in Figure 3.1. The seizure features closely resemble the non-seizure features; thus, making it almost impossible to discriminate between the two classes, causing the detector to fail to recognize a seizure event. Furthermore, the resemblance of the seizure and non-seizure features increases the burden on the detector to differentiate between the seizure and non-seizure features and often increases the number of false detections or severely decreases the sensitivity of the detector. Figure 3.12 depicts the extracted features from the β-frequency band of the EEG record shown in Figure 3.2 (after CSP feature enhancement). The energy in the non-seizure data is greatly attenuated and the seizure features are clearly

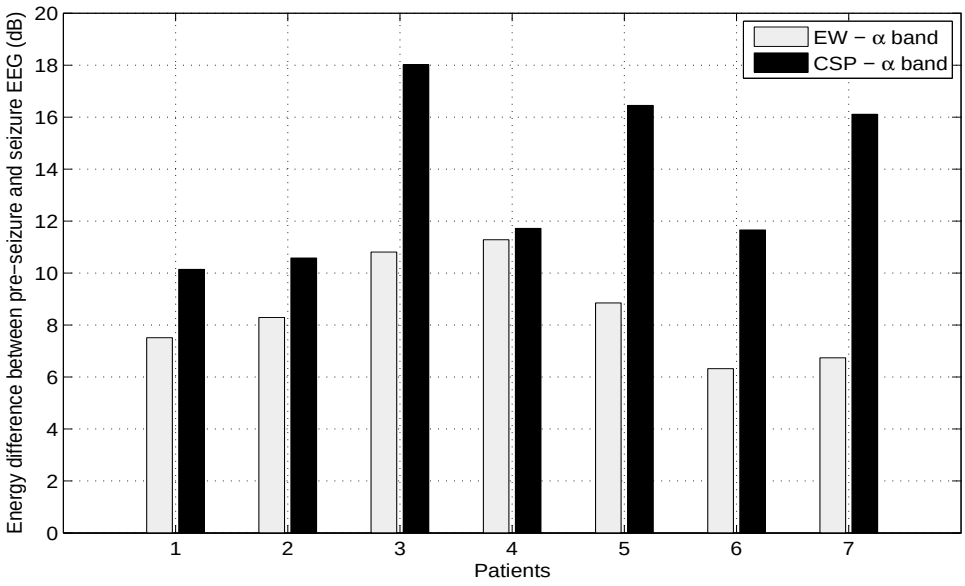

Figure 3.6: Average difference in energy between the pre-seizure and seizure EEG in the α frequency sub-band.

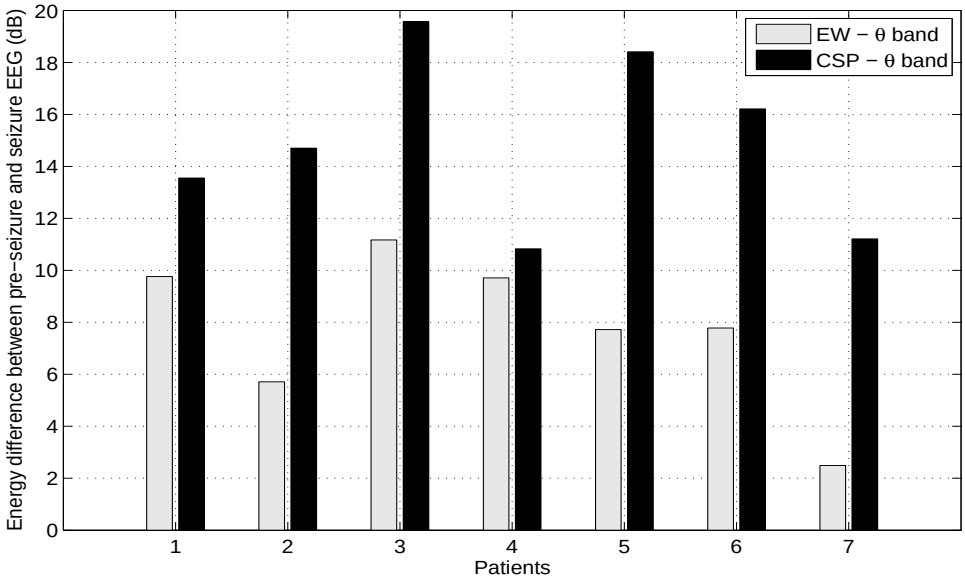

Figure 3.7: Average difference in energy between the pre-seizure and seizure EEG in the θ frequency sub-band.

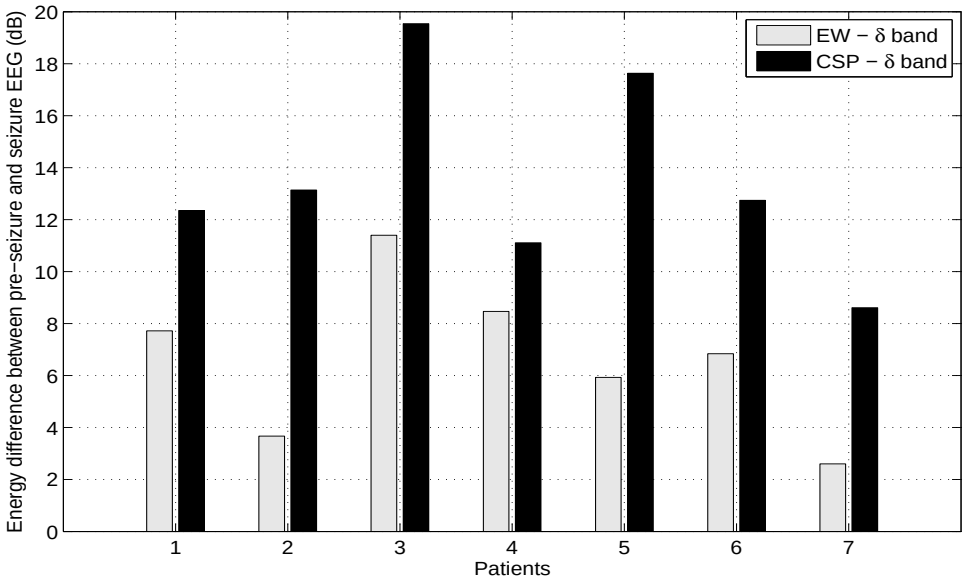

Figure 3.8: Average difference in energy between the pre-seizure and seizure EEG in the δ frequency sub-band.

distinguishable from the non-seizure features.

Another example to illustrate the success of the feature enhancement unit is shown in Figs. 3.11 and 3.12. Figure 3.11 depicts the energy in the θ-frequency band when feature extraction is done on the EEG waveform in Figure 3.3, and Figure 3.12 depicts the extracted features from the θ-frequency band of the EEG record shown in Figure 3.4 after CSP feature enhancement. The effect of the feature enhancement stage is evident by visual comparison.

3.3 Performance Evaluation of the EEG-based SOD

In this section, performance evaluation results of the proposed detectors are presented and discussed. In these simulations, we compare the performance of the proposed detectors to other detection systems that: 1) do not employ a channel selection stage (e.g., [16],[27], [28], [40], [41], [42]), 2) do not employ a feature enhancement stage (e.g.,[16],[27], [32], [40], [41], [42]), 3) adopt a feature enhancement

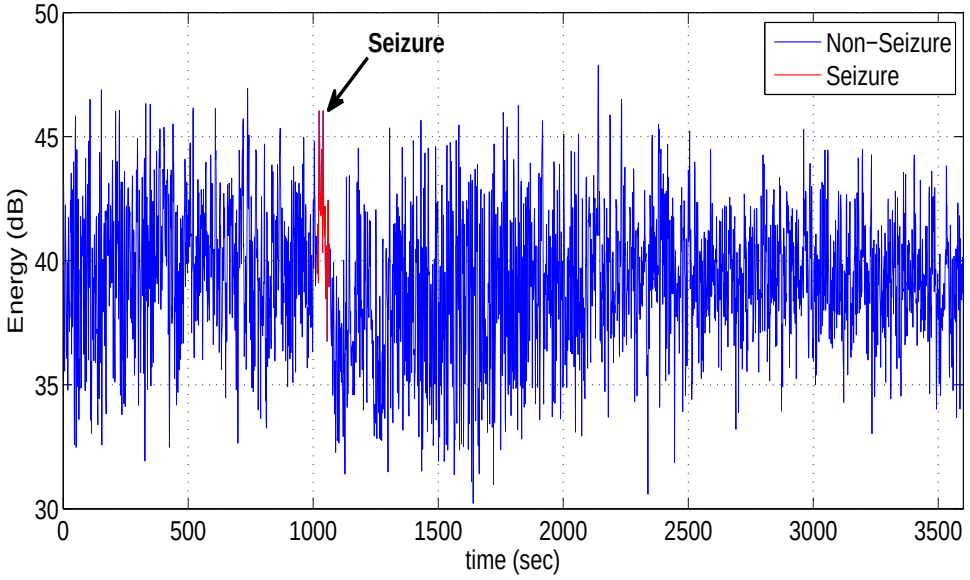

Figure 3.9: Energy contained in the β frequency band after EWSA of a seizure record of patient 1. Seizure features are shown in red and are marked by the arrow. Non-seizure features are shown in blue.

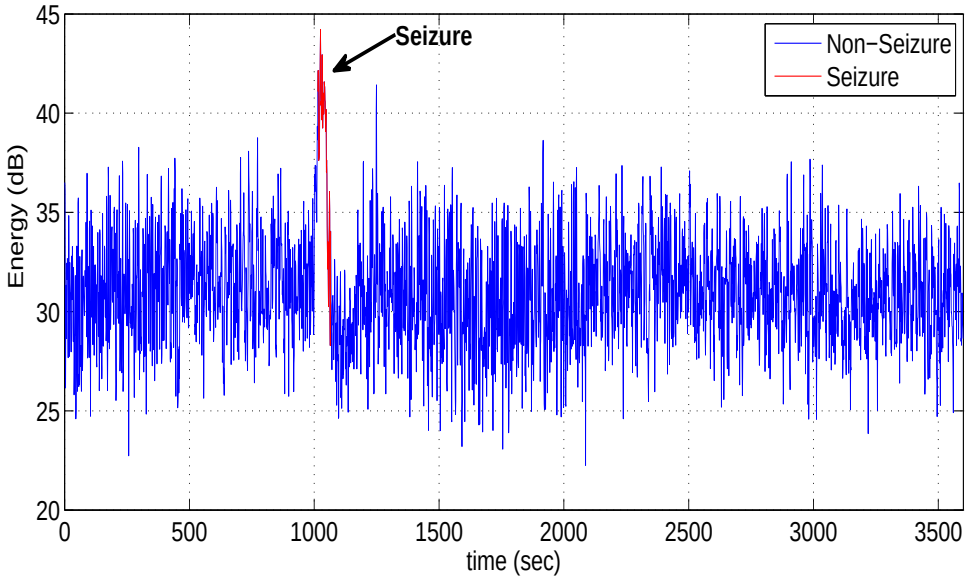

Figure 3.10: Energy contained in the β frequency band after CSP of a seizure record of patient 1. Seizure features are shown in red and are marked by the arrow. Non-seizure features are shown in blue.

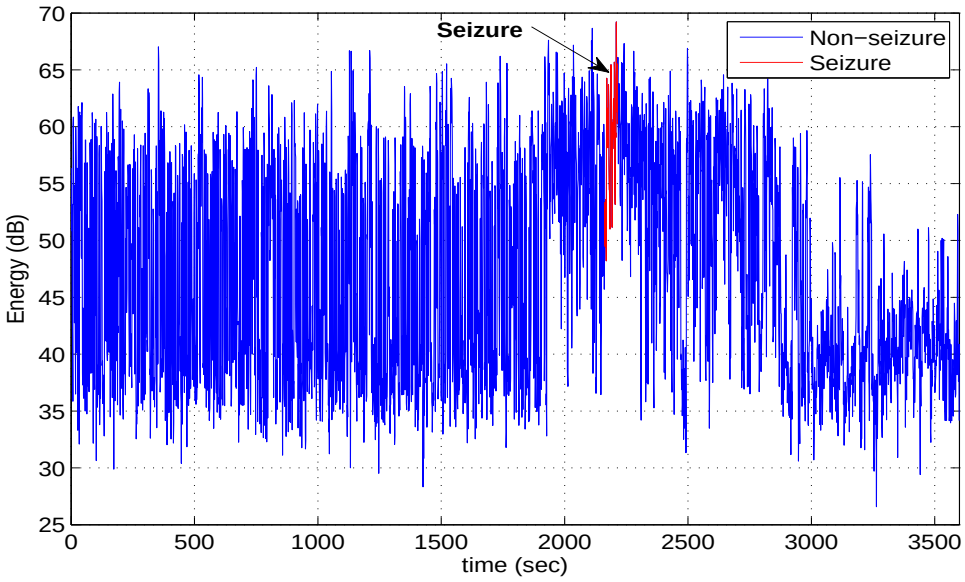

Figure 3.11: Energy contained in the θ frequency band after EWSA of a seizure record of patient 3. Seizure features are shown in red and are marked by the arrow. Non-seizure features are shown in blue.

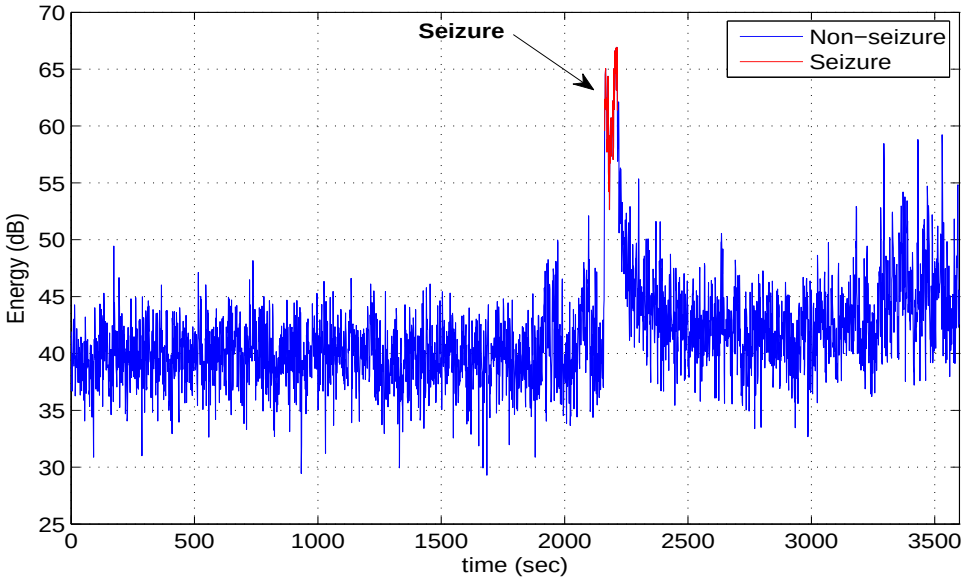

Figure 3.12: Energy contained in the θ frequency band after CSP of a seizure record of patient 3. Seizure features are shown in red and are marked by the arrow. Non-seizure features are shown in blue.

stage that is not based on CSP and do not employ a channel selection stage (e.g., [28]), 4) adopt a channel selection stage without a feature enhancement stage (e.g., [32]), 5) adopt a single SVM classification stage (e.g., [16],[27], [32], [28], [40], [41], [42]]), 6) adopt a pre-processing stage to remove artifacts (e.g., [27], [41]), 7) use the same clinical data set for testing (e.g., [16]), and 8) commercially available, i.e., a standard detector (e.g., [43]).

3.3.1 Testing Methodology and Performance Measures

To test the proposed detectors, a leave-one-out cross-validation testing scheme is adopted for each subject. In the leave-one-out cross-validation testing scheme, the SVM is given a training set that includes the seizure and non-seizure epochs from all but one of the subject's recordings. The detector then attempts to detect the seizure epochs from the excluded record using the learned knowledge from the training set. This is repeated until each recording from the subject is excluded once.

Each subject's EEG recording undergoes channel selection and CSP filtering using the chosen channels and extracted CSP filters from an independent EEG recording that is not used in the training or the testing recordings. This record is only used to select the N_{ch} channels with the most valuable seizure-related information and to extract the CSP filters for that particular patient.

The performance of the proposed detectors is characterized in terms of the detection latency, number of false alarms per hour, and sensitivity. *Detection latency* (DL) refers to the delay between the electrographic seizure onset marked by the electroencephalographer and a seizure event declared by the detector. The detection latency accounts for the timing constraint T_c. The *number of false alarms per hour* (FA/hr) is the number of times the detector declares the onset of a seizure in the absence of an actual seizure. *Sensitivity* (S) refers to the percentage of seizures

correctly identified by the detector.

3.3.2 Performance of the Proposed TC-SOD

The performance of the TC-detector in terms of sensitivity, detection latency, and false alarm rate per hour is shown in Table 3.1 for several patients. It is evident that patient 2 performs the worst in terms of sensitivity and false alarm rate per hour. The reason behind the poor performance is because certain frequency bands of the patient EEG present minimum separation between seizure and non-seizure events, causing the detector to fail to detect some seizure instances as well as increasing the detection latency. However, the performance of the detector with the remaining patients achieves 100% sensitivity and low detection latency and false alarm rates.

Table 3.1: TC-Detector Performance

Patient	**S (%)**	**DL (sec)**	**FA / hr**
1	100	0.66	0.5
2	66.67	19.33	1
3	100	8.25	0
4	100	4.8	0.5
5	100	3	0.11
6	100	7.25	1.87
7	100	1.75	0.15

3.3.3 Performance of the Proposed BS-SOD

Table 3.2 shows the performance of the BS-detector for several patients and for different fusion methods. The proposed detector achieves 100% sensitivity for all patients in all three fusion methods. More specifically, the detector successfully detects all seizures from all patients using all the fusion techniques. Analyzing each patient separately, it is evident that the OR fusion method yields the highest false alarm rate compared to the AND and MAJ methods. Such a performance is intuitive

since for the OR fusion technique, a global seizure event is declared if SVM declares only one seizure event in any of the frequency bands. Therefore, normal, seizure-like activity observed in particular frequency bands will trigger the system to initiate a seizure alarm, when in fact no seizure is present. On the other hand, the OR method is able to detect the onset of a seizure in the shortest amount of time since this method is sensitive to any seizure alarm in any frequency band.

Table 3.2: BS-Detector Performance

Patient	**S (%)**			**DL (sec)**			**FA / hr**		
	AND	**OR**	**MAJ**	**AND**	**OR**	**MAJ**	**AND**	**OR**	**MAJ**
1	100	100	100	2.16	0	0.66	0.25	12.06	2.5
2	100	100	100	27.33	10.33	12	0	4.81	0.5
3	100	100	100	9	0.75	5	0.06	4.06	0.43
4	100	100	100	27	2.6	17.8	0.22	4.33	0.44
5	100	100	100	4	1	3.5	0.51	6.08	1.08
6	100	100	100	10	0.25	9	1.06	4.81	2.25
7	100	100	100	8	1.25	3	0.07	4.81	0.33

For Tables 3.1 and 3.2, the false detections of patient 6 are caused by non-physiological artifacts. All other false detections in the performance tables are caused by periodic discharges that closely resemble the seizure onset of the subject and exceed 6 seconds in duration, such as IEDs. These false alarms may, in fact, have been *mini-seizures*. These false detections can be avoided by forcing the detector to declare a seizure event only in the presence of seizure activity for 8 or 10 seconds ($T_c = 4$ or $T_c = 5$). The cost of such a modification would be an increase in the average detection latency.

3.4 Comparison with State-of-the-Art SODs

Table 3.3 shows the mean performance of the TC-detector and BS-detector over all patients. The BS-detector is able to detect all of the patients seizure with a latency ranging from 2.31 seconds for the OR fusion method to 12.5 seconds for the AND fusion method. The MAJ fusion technique achieves a good compromise between delay and false alarm rate as compared with the AND and OR fusion techniques. Compared with TC-detector, the BS-detector achieves higher sensitivity with comparable results for the delay and false alarm rate in case of the MAJ fusion technique.

Table 3.3 also compares the performances of the proposed detectors with several state-of-the-art seizure onset detectors. The detectors in [27] and [41] both adopt different pre-processing steps before detection in order to rid the EEG from noise and artifacts. The proposed detector in [16] uses the same patient database as the one described in Section 3.1. Furthermore, the extraction of the features is done in a similar manner to Section 2.2.3. As a result, the detector [16] is analogous to the TC-detector while omitting the channel selection and feature enhancement stages. The detector in [28] uses the method of signal differentiation as a feature enhancement method but does not assume any form of channel selection. The detection algorithm in [40] extracts temporal and spectral features from iEEG channels. The spectral features of the iEEG are extracted by sliding one-second intervals of the iEEG waveform through a filter bank and then measuring the energy falling within the passband of each filter. The detector in [32] uses the same channel selection method adopted in this work. The selected channels then undergo the same feature extraction process as in Section 2.2.3. The detector in [43] is developed by NeuroPace Inc. and is commercially available. The detector in [44] is an FDA approved seizure onset detector developed by Optima Neuroscience. The proposed detectors in this

work achieve the best sensitivity results when compared with the existing detectors shown in Table 3.3. Furthermore, the proposed detectors, on average, perform better in terms of detection latency than the detectors proposed in literature.

3.4.1 Proposed SODs and their Clinical Relevances

Seizure onset detection is particularly useful to neurologists who usually spend hours analyzing patients' EEG records in an attempt to locate a seizure. Automatic seizure detection systems, such as the proposed EEG-based SOD, greatly reduce the volume of data that must be analyzed by doctors. However, these systems are required to be highly sensitive, even if the false alarm rate is high. The reason is that neurologists are in general capable to easily cast out false alarms from the detectors results by reviewing the suspicious alarms. The BS-detector is ideal for neurologists to identify a seizure since it achieves 100% sensitivity. In this regard, the AND fusion technique is the best fusion method since it achieves high sensitivity with the lowest false alarm rate and has an acceptable delay performance (delay here is not an issue since neurologists are usually working off-line).

In addition, SODs are gaining more attention as possible seizure control devices. Such detectors can control seizures by initiating anti-epileptic drugs or by selectively stimulating certain parts of the brain when an oncoming seizure is detected. In a hospital setting, such a device would be useful in initiating time-sensitive clinical procedures necessary for the investigation of various epileptic characteristics, such as localizing a patient's epileptogenic focus via ictal-SPECT or fMRI. Seizure prevention applications require high sensitivity and low false alarm with minimum delay. In this regard, both the TC-detector and the MAJ fused BS-detector perform optimally with respect to sensitivity compared to the state-of-the-art detectors and offer a good compromise between sensitivity, false alarm, and detection latency.

Table 3.3: Average Detector Performances

Detector Architecture		S (%)	DL (sec)	FA / hr	Length of data (hrs)
TC-detector		95.2	6.43	0.59	90
BS-detector	**AND**	100	12.5	0.35	90
	OR	100	2.31	6.03	90
	MAJ	100	7.28	1.2	90
[**42**]		90.15	n/a	0.03	95
[**41**]		73.9	n/a	0.15	1475
[**27**]		75.8	10	0.09	95
[**32**]		96	n/a	0.14	1419
[**28**]		89.8	9.2	0.125	428
[**40**]		97	5	0.6	875
[**16**]		94.2	8 ± 3.2	0.25	60
[**43**]		97	5.01	0.013	200
[**44**]		80	n/a	0.086	1208

4. ECG-BASED SEIZURE ONSET DETECTION

In this chapter, the components making up the ECG-detection unit, shown in Figure 4.1, are presented in detail. In particular, the steps taken to extract the HRV information from ECG are discussed, the quadratic TF algorithm is analyzed, and the feature extraction and classification steps are presented. Also, the performance of the ECG-based detector on a set of clinical patients is presented.

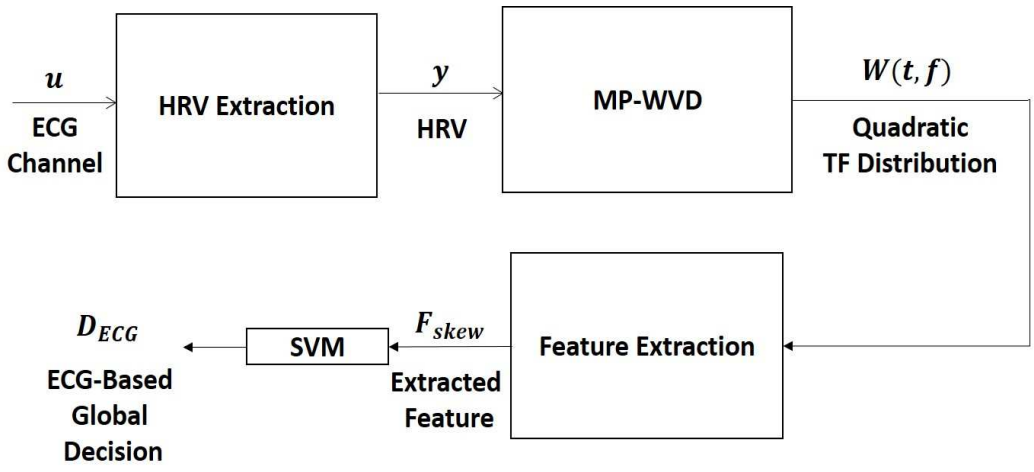

Figure 4.1: An illustration of the ECG-based SOD architecture.

4.1 HRV Extraction

This section presents the different steps required to obtain the HRV from raw ECG. The steps are illustrated in Figure 4.2.

The first step addresses the problem of baseline wander in the ECG data. ECG baseline correction in this work is done via a robust and computationally efficient, iterative algorithm termed Baseline Estimation and Denoising with Sparsity (BEADS)

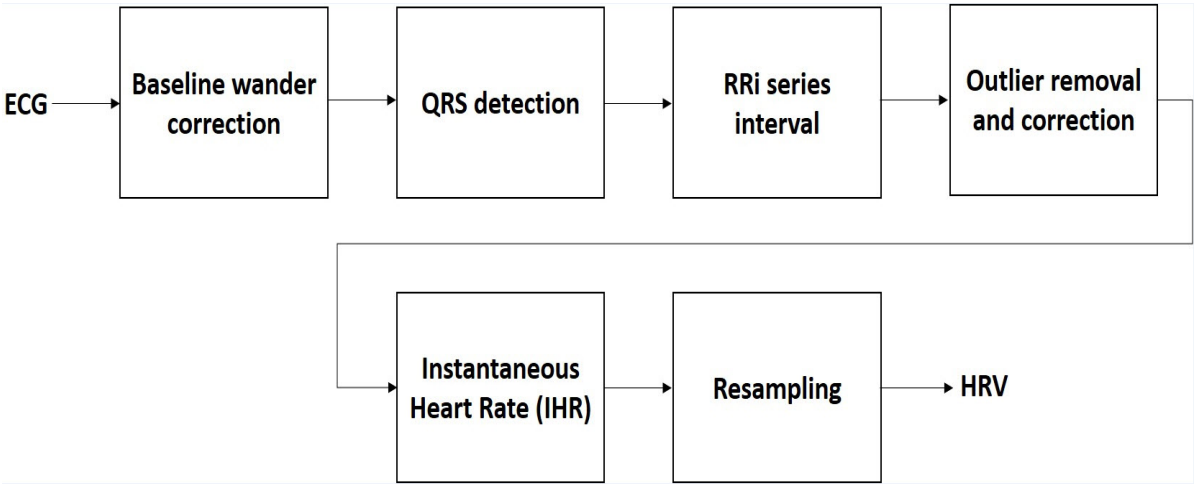

Figure 4.2: HRV extraction process.

[45]. The second step is implementing a QRS detection algorithm that detects QRS complexes and localizes R-waves. The algorithm works by searching for local maxima that are above a certain predefined threshold value. The threshold value ensures that the R-peaks are detected instead of the P- and T-wave maxima. Once an R-peak is detected, the algorithm waits for a period of Δ_R seconds before searching for a consecutive R-peak. The wait period is adopted to avoid misclassification due to noise. The R-peaks are taken as the location of the R-points. Next, the time duration between consecutive R-peaks is used to represent the heart's beat-to-beat interval. This series is known as the RR interval time series, RRi, or tachogram.

The next step in the HRV extraction stage is the removal of outliers from the RRi data. Outliers may exist in the RRi due to QRS missed detections, false detections, ectopic beats, or other random-like physiological disturbances. In general, outliers are defined as values which are not within a specified limited interval. In the context

of HRV extraction, outliers are defined as [46]:

$$Outlier(n) = \begin{cases} RRi(n) & \text{if} \quad RRi(n) < 1^{st} \text{ quartile}(RRi) - \\ & \quad \text{interquartile\_range}(RRi) \times \eta \\ RRi(n) & \text{if} \quad RRi(n) > 3^{rd} \text{ quartile}(RRi) + \\ & \quad \text{interquartile\_range}(RRi) \times \eta \end{cases} \tag{4.1}$$

where $0 < n \leq \text{length}(RRi)$ and η is a constant. For our data, η is chosen to be 7. Once the outliers are identified, they are removed and the missing data is spline interpolated.

An instantaneous heart rate (IHR) signal is obtained by taking the inverse of the RRi signal. The IHR signal is not uniformly sampled. In the case of time-domain analysis, it is not an issue; however, time-frequency analysis assumes the signal to be uniformly sampled. Therefore, the IHR signal is then uniformly sampled through the method of linear interpolation to obtain a new uniform sampling rate of 20 Hz. The resulting signal, y, constitutes the HRV signal.

4.2 MP-WVD Algorithm

This section outlines the methods used to generate a high-quality TF distribution of the HRV signal.

The main idea of the quadratic TF distribution is to distribute the energy of a signal along the time and frequency domains. In this work, the WVD quadratic transform is investigated. The WVD satisfies several desirable mathematical properties; namely, it is real valued, it preserves time and frequency shift information contained in the signal of interest, it satisfies the marginal properties, the frequency integral of the WVD corresponds to the signal's instantaneous power, and the instantaneous frequency can be estimated from the first moment of the WVD [47].

Although the WVD has good theoretical properties, its major drawback is that it can suffer from interference terms (or cross terms) between the components of a multi-component signal. These interference terms oscillate in the TF plane and indicate activity which does not exist, leading to erroneous visual interpretation of a signal's TF structure. To partially reduce the interference terms, the analytic signal can be used in the WVD algorithm. Windowed versions of the WVD have been proposed to reduce the interference terms; namely, the pseudo-WVD (PWVD) and the smoothed-pseudo-WVD (SPWVD) [48]. However, these methods present a trade-off between TF resolution and cross-term reduction and they only *reduce* the interference terms; they do not *eliminate* them. Because interference terms in the WVD appear only in multi-component signals, we implement an algorithm that decomposes the HRV signal into a sum of mono-component signals. This decomposition can be carried over by employing the MP algorithm.

The MP algorithm decomposes a signal into a sum of atoms from a given dictionary. In this work, the Gabor atom dictionary is used because Gabor atoms are mono-component signals per definition. Therefore, the application of the WVD on a signal that has been decomposed via MP with Gabor atoms does not yield any interference terms and presents excellent time-frequency resolution. The Gabor atom can be expressed in terms of the modulated Gaussian function $g(t) = e^{-\pi t^2}$. The Gabor atom assumes the expression [49]:

$$g(t) = Ae^{-\pi\left(\frac{t-h}{s}\right)^2} cos\left(f_m(t-h) + \varphi\right)) \tag{4.2}$$

where s represents a scaling factor, f_m denotes the frequency modulation, h stands for the translation factor, φ models the phase, and A is a normalization factor such that $\|g(t)\| = 1$. Let D represent the Gabor atom dictionary such that

$D = [g_1(t), g_2(t), \cdots g_M(t)]$, where M denotes the number of atoms in the dictionary. The MP decomposition of the HRV signal $y(t)$ is expressed as:

$$y(t) \approx \sum_{n=1}^{N} a_n g_n(t) + R_N, \tag{4.3}$$

where $M \gg N$, a_n is a weighting coefficient, and R_N denotes the residual. The MP decomposes $y(t)$ by finding the best orthogonal projections amongst a set of basis functions from the dictionary D that matches the structure of $y(t)$. The result is a finite number of basis functions organized in a decreasing order of energy. The standard MP algorithm is an iterative algorithm and is outlined in the following steps.

Step 1: Initialize $n = 1$ and $R_0 = y(t)$.

Step 2: Compute $|\langle R_{n-1}, g_i(t)\rangle|$ for all $g_i(t)\ \epsilon\ D$.

Step 3: Find $g_n^* = \underset{g_i(t)}{\operatorname{argmax}} |\langle R_{n-1}, g_i(t)\rangle|$.

Step 4: Compute the weighting coefficient: $a_n = \langle R_{n-1}, g_n^*\rangle$.

Step 5: Compute the new residual: $R_n = R_{n-1} - a_n \cdot g_n^*$.

Step 6: Remove g_n^* from D.

Step 7: If $n = m$ or $\epsilon \leq threshold$, stop, where m is a given iteration number and ϵ is the energy of the residual R_n; otherwise set $n = n + 1$ and go to **Step 2.**

Let the MP-decomposed HRV signal be denoted by $y_{MP}(t)$, then the WVD of $y_{MP}(t)$ is given by

$$W(t, f) = \int_{-\infty}^{+\infty} y_{MP}\left(t + \frac{\tau}{2}\right) y_{MP}^*\left(t - \frac{\tau}{2}\right) e^{-j2\pi f\tau} d\tau, \tag{4.4}$$

where the values of $W(t, f)$ are stored into an $\mathrm{L}_t \times \mathrm{L}_f$ matrix and the asterix symbol used as a superscript indicates the operation of complex conjugation. With these combined algorithms, the MP-WVD approach provides excellent TF resolution of the HRV signal without any interference terms.

4.3 Feature Extraction and Classification

There are many features that can be extracted from the TF distribution of the HRV signal to characterize the seizure and non-seizure phenomena, such as central frequency, mean, skewness, kurtosis, and Shannon entropy [50], [47] . In this work, the skewness of MP-WVD HRV signal is chosen because, based on our experimental analysis, skewness best characterizes changes in epileptic HRV. Skewness is a time-domain feature that can be translated to the TF domain as follows [50]

$$F_{skew} = \frac{1}{(L_t L_f - 1)\sigma_{TF}^3} \sum_{i=1}^{L_t} \sum_{j=1}^{L_f} \left(W[i,j] - \mu_{TF}\right)^3, \tag{4.5}$$

where μ_{TF} and σ_{TF} are the mean and standard deviation of $W(t, f)$ and are given by

$$\mu_{TF} = \frac{1}{L_t L_f} \sum_{i=1}^{L_t} \sum_{j=1}^{L_f} W[i,j] \tag{4.6}$$

and

$$\sigma_{TF}^2 = \frac{1}{L_t L_f} \sum_{i=1}^{L_t} \sum_{j=1}^{L_f} \left(\mu_{TF} - W[i,j]\right)^2, \tag{4.7}$$

respectively. Once F_{skew} is extracted, it is classified as a seizure or non-seizure feature by a SVM that has been trained on features of the same nature. In an attempt to decrease the number of false seizure detections, a timing constraint, T_c, is adopted. The timing constraint prevents the ECG-based detector from declaring a seizure event until the SVM has detected T_c consecutive seizure epochs. The same timing

constraint as in the EEG-based SOD is adopted, $T_c = 3$.

4.4 Performance Evaluation of the EEG-based SOD

In this section, the performance of the proposed ECG-based SOD is presented and discussed.

4.4.1 Clinical Data

The data used to evaluate the ECG-based SOD detector is obtained from the EPILEPSIAE project [51]. The data was recorded during pre-surgical epilepsy monitoring at the Epilepsy Center of the University Hospital of Freiburg in Germany. The dataset includes 10 patients where each patient has between 98 to 280 continuous EEG and ECG recordings and exhibits between 5 to 22 seizures. All signals are sampled at 256 samples per second with 16-bit resolution. The International $10-20$ System of EEG electrode positions and nomenclature is used for these recordings. All recordings have 19 EEG channels and one-lead ECG recording.

Each seizure's electrographic onset is marked by an experienced electroencephalographer and corresponds to the onset of a rhythmic activity that is associated with a clinical seizure. Each seizure's clinical onset time is also recorded. The data is segmented into one-hour-long records. Records that do not contain a seizure are referred to as non-seizure records and those that contain one or more seizures are referred to as seizure records. Furthermore, the recordings are made in a routine clinical environment, so non-seizure activity and artifacts such as head/body movement, chewing, blinking, early stages of sleep, and electrode pops/movement are present. No constraints regarding the types of seizure are imposed; the data set contains complex partial (CP), simple partial (SP), and secondary generalized seizures (GS). Table 4.1 summarizes the clinical data used in our performance evaluation.

No form of pre-processing for artifact and noise removal has been performed on

the data. Our approach to deal with artifacts is based on training our detector to recognize artifacts, rather than actively removing them using standard signal processing techniques.

Table 4.1: Summary of Clinical Data used in Performance Evaluations

Patient No.	Age	Gender	Type of Seizure	No. of Recordings	No. of Seizures
1	36	Male	CP	172	11
2	52	Female	SP	281	8
3	36	Male	SP	121	5
4	43	Female	SP & CP	130	8
5	65	Male	SP, CP, & GS	138	8
6	26	Male	SP	117	22
7	47	Male	CP & GS	98	6

4.4.2 MP-WVD TF-Analysis

The HRV of patient 1 one-hour ECG data is depicted in Figure 4.3. The blue signal corresponds to the non-seizure HRV data and the red signal is the seizure HRV data. The seizure starts at 2638 seconds and lasts until 2693 seconds. This particular patient observes a sharp decrease of HRV after the onset of the seizure, reaching 0.95 beats per second (bps). Figure 4.4 illustrates the MP-WVD of a segment of the HRV taken 20 seconds prior to the seizure onset and 20 seconds after the seizure offset. The HRV time-domain signal is also shown in Figure 4.4 for discussion purposes. In this segment, the seizure onset and offset are marked by arrows. Approximately ten seconds after the onset of the seizure, activity in the low-frequency band (0.04-0.15 Hz) is noticed, followed by a sharp decrease of spectral activity in the very low frequency band (0.0033-0.04 Hz). This activity coincides with the decrease in HRV that occurs 33 seconds after the onset of the seizure. The skewness, calculated from the MP-WVD of the HRV shown in Figure 4.3, is depicted in Figure 4.5. The

skewness of the HRV decreases after the onset of the seizure and resumes normal activity after the seizure episode has passed. Visually looking at the graph of the skewness feature, we are able to detect the unusual activity from the background features.

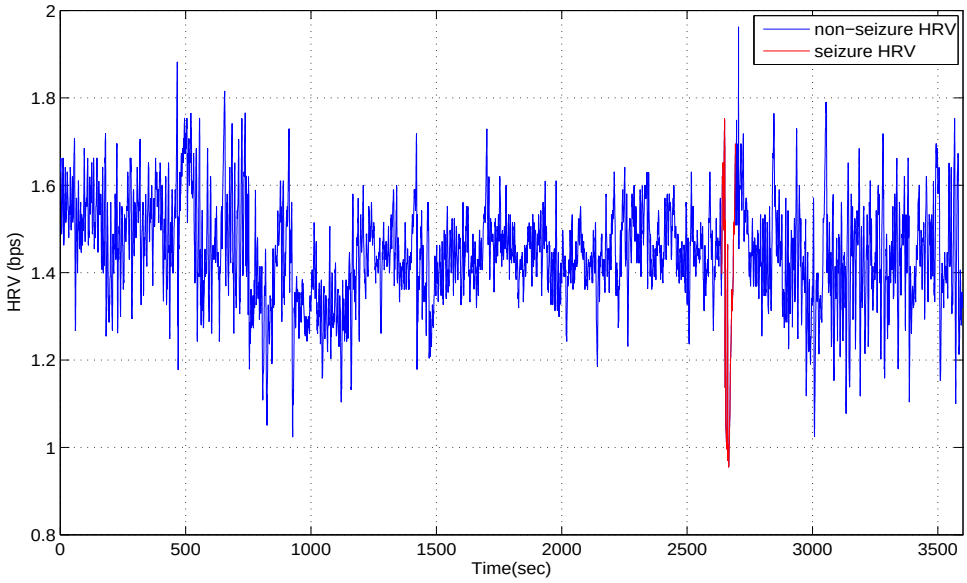

Figure 4.3: HRV of patient 1.

4.4.3 Performance Assessment with State-of-Art SODs

The performance of the ECG-based detector is given in Table 4.2. The detector achieves an average sensitivity of 96.4% and has an average FA/hr of 5.4 seconds. The DL seems a bit higher than what would be desired. This is explained by investigating how different types of seizures affect HRV. A study carried out by [52] shows that ictal tachycardia (ITC) is an ictal phenomenon rather than a pre-ictal phenomenon and the onset of ITC varied between 21.6 and 23.7 seconds from the seizure onset in ECoG. Therefore, the resulting DL of the ECG-based SOD reflects the findings in [52].

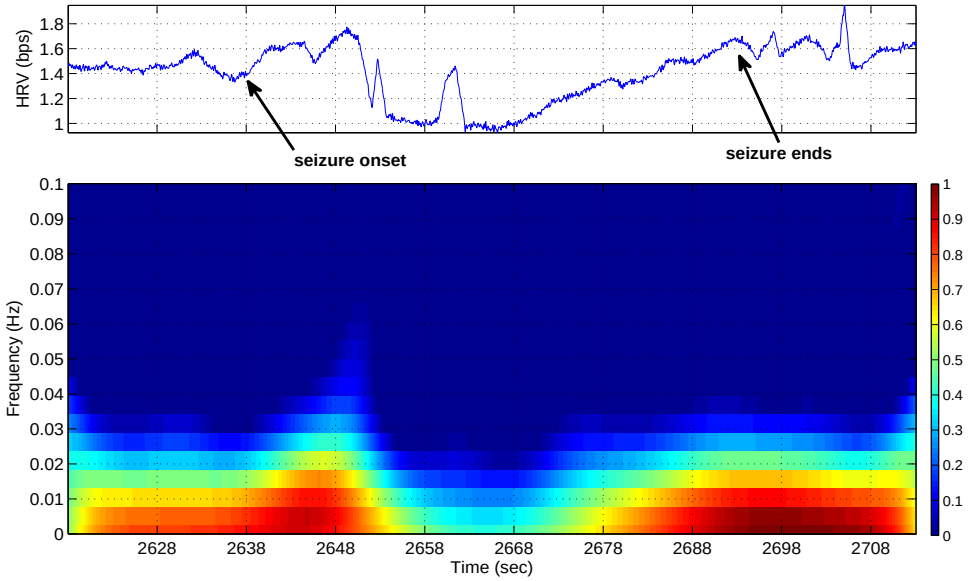

Figure 4.4: Segment of MP-WVD of the HRV of patient 1. Color bar in $(\text{bps})^2$.

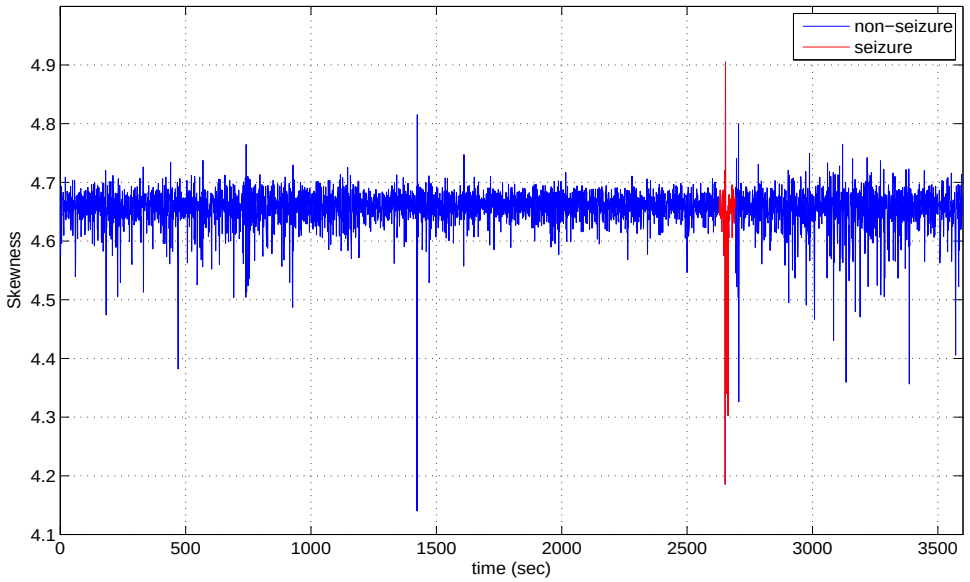

Figure 4.5: Skewness of the MP-WVD HRV of patient 1.

Table 4.2: ECG-Based Detector Performance

Patient No.	FA/hr	DL (sec)	Sensitivity (%)
1	9.5	20.5	100
2	1.5	8.25	100
3	3	15	100
4	9	8	75
5	6	12	100
6	5	8	100
7	3.5	10	100
Avg	5.4	13.1	96.4

Table 4.3 compares the performances of the proposed ECG-based detector with several ECG-based state-of-the-art seizure onset detectors. An extra performance criterion, specificity, is added for comparison to state-of-the-art detectors that provide only specificity measures instead of a FA rate. The specificity is defined as

$$Specificity = \frac{TN}{TN + FP}, \tag{4.8}$$

where TN is the amount of true negatives and FP is the amount of false positives.

The detector in [53] analyzes HRV using four different HRV methods with short term moving window analysis. In [12], ten time-domain and frequency-domain features are extracted from HRV and classified using an Artificial Neural Network (ANN). The detector in [36] is based on the fusion of HRV-based decision and EEG-based decision. The detector extracts time-domain features from HRV and spectral features from EEG to detect neonatal seizures. The proposed ECG-based SOD obtains the highest sensitivity and specificity level. No information has been released regarding the FA/hr for [12] and [53] and regarding the DL for [12].

Table 4.3: Comparison of Average Detector Performances

Detector Architecture	FA/hr	DL (sec)	Sensitivity (%)	Specificity (%)
ECG-based Detector	5.4	13.1	96.4	99.85
[53]	n/a	14	76.64	n/a
[12]	n/a	n/a	88.66	90

5. EEG-ECG FUSED SEIZURE ONSET DETECTION

This chapter outlines the procedure of fusing the ECG-based and EEG-based decisions to yield a single detection decision. Two different fusing techniques are analyzed and the proposed detector is tested on a set of clinical patients. Results are discussed and compared to existing state-of-the-art SODs. Fig. 5.1 illustrates the EEG-ECG fused SOD, where the EEG-based detector and the ECG-based detector are outlined in Chapters 2 and 4, respectively.

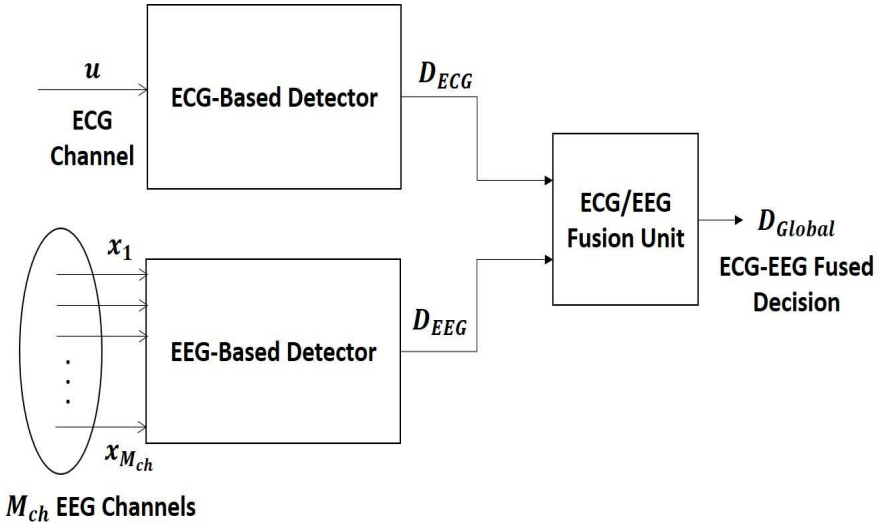

Figure 5.1: An illustration of the ECG-EEG fusion SOD architecture.

5.1 Benefits of Using a Second Biosignal

As discussed in Chapter 1, seizures are characterized by the hyperactivity and hypersynchrony of neurons in the brain. Scalp EEG is able to record the neural activity on the cerebral cortex. However, when the underlying neural hypersynchrony

involves neural networks deep within the brain, scalp EEG may not be able to pick up on these signals, but instead display physical consequences of the seizure, i.e., rapid eye-blinks, muscle contractions, and altered senses. Only when the epileptic neural discharge is large enough, rhythmic activity that reflects the epileptic neural hypersynchrony manifests within the EEG.

These types of seizures pose serious challenges in terms of seizure detection using only EEG. Additional information derived via a secondary biosignal whose dynamics are influenced by epileptic seizures can aid in seizure detection. The fusion of EEG and a secondary biosignal will complement each other in terms of seizure detection. We have chosen to fuse the ECG signal since HRV has shown to be a good measure for seizure detection, as shown in Chapter 4. Patient-specificity remains essential to the success of this approach since the manner with which the scalp EEG and ECG change during seizure and non-seizures states varies across patients.

5.2 Fusion System 1: Always Fuse

In the always fusion (AF) system, the decisions from the EEG-based, D_{EEG}, and ECG-based, D_{ECG}, detectors are fused directly to obtain the detector's final decision, D_{Global}. In this system, D_{Global} can only be a seizure output if and only if D_{ECG} and D_{EEG} are both seizure outputs, otherwise the detector's global decision will be a non-seizure output decision. Mathematically, this can be represented by

$$D_{Global} = \begin{cases} 1 & \text{iff} \quad D_{EEG} = D_{ECG} = 1 \\ 0 & \text{otherwise} \end{cases}, \tag{5.1}$$

where 1 denotes a seizure decision and 0 denotes a non-seizure decision.

This system is particularly useful in situations in which the EEG signal suffers from artifacts similar to seizure manifestations which, in return, increases the number

of false alarms. As will be shown in Section 5.4, the AF system decreases the total number of false alarms compared to the EEG-based detection system.

5.3 Fusion System 2: Over-ride Fuse

The second fusion system is termed the over-ride fusion (OF) system. It implements the AF system with an additional over-ride option. The over-ride option over-rides the AF system and allows the global deceleration of a seizure when the detector observes T_{ovr} consecutive *seizure* global EEG decisions. In this work, $T_{ovr} = 5$. The over-ride option is useful in situations where ECG seizure manifestations are observed 15-20 seconds into a seizure. This study, as well as the study in [52], show that ITC is an ictal rather than a pre-ictal phenomenon, specifically in patients with temporal lobe epilepsy (TLE). Therefore, in addition to decreasing the number of false alarms relative to an EEG-based detector, the OF detection system also allows for the early detection of seizure onset in situations of late-ictal ECG onset.

5.4 Performance Results of the Fused EEG-EEG SOD

In this section, the performances of the proposed fusion detectors are presented and discussed. We compare the performance of the proposed detector to other detection systems that: 1) employ an EEG-based detector only, with no channel selection stage (e.g., [28], [40]), 2) employ and EEG-based detector with no feature enhancement stage [40]), 3) employ an EEG-based detector using a single SVM classification stage (e.g., [28], [12], [35], [36], [40], [53]), 4) employ an ECG-based detector using time- or frequency-domain features (e.g., [12], [53]), 5) employ EEG and ECG fusion detection using time- or frequency domain features (e.g., [35], [36]), and 6) with commercially available detectors (e.g., [43], [44]).

5.4.1 Performance of Proposed Fusion Detectors Compared with Stand-Alone Detectors

The testing methodology and clinical dataset in this chapter are identical to that in Chapter 4.

The performances of stand-alone EEG-based and ECG-based detectors on the same dataset as in Section 4.4.1 are given in Tables 5.1 and 5.2, respectively. These performances are computed so that we are able to quantify the enhanced performance of the fused detectors compared with EEG-based or ECG-based detectors. The performance of the proposed AF detector is given in Table 5.3. The AF detector achieves 100% sensitivity and has a lower FA rate than both the EEG- and the ECG-based detectors. Specifically, the AF system observes an improvement of 79% for the AND EEG sub-band fusion compared with the EEG stand alone system and 83% improvement compared with the ECG stand alone system. The AND EEG sub-band fusion technique yields the lowest FA rate because of its stringent criteria for all four sub-band decisions to yield a seizure detection before the proclamation of a seizure; however, this comes at the expense of a slightly higher DL. The OR EEG sub-band fusion technique achieves the smallest DL at the expense of a higher FA rate. The MAJ EEG sub-band fusion technique is a compromise between the AND and OR fusion techniques. The detection latency of the AF detector is higher than the EEG-based detector due to the ECG fusion. A study carried out by [52] shows that ITC is an ictal phenomenon rather than a pre-ictal phenomenon and the onset of ITC varied between 21.6 and 23.7 seconds from the seizure onset in ECoG.

The AF detector is particularly useful to neurologists who analyze patients' EEG records in an attempt to locate seizure instances. Once again, in these situations, automatic seizure detection systems must favor high sensitivity over low DL and FA

rates because neurologists are, in general, capable of easily casting out false alarms from the detectors results by reviewing the suspicious alarms, and are able to easily locate ictal onset in short segments of physiological data. Therefore, in this instance the AND-fusion technique is the best since it achieves high sensitivity with the lowest false alarm rate (again, here delay is not an issue since neurologists normally work off-line).

The performance of the OF detector is shown in Table 5.4. The over-ride option allows for excellent DLs with the trade-off of slightly higher FAs. The MAJ fusion technique, in the case of this detector, offers the best trade-off between the DL and FA rate while still achieving 100% sensitivity. In comparison with the stand alone systems, an improvement of 27.9% for the AND EEG sub-band fusion is observed compared with the EEG stand alone system and 44% improvement compared with the ECG stand alone system. This detector is suitable for online detection of seizure onset because of the small DL time and high sensitivity.

In terms of seizure warning and prevention applications, these systems require high sensitivity and low false alarm with minimum delay. In this regard, the proposed OF detector performs optimally and offers a good compromise between sensitivity, false alarm, and detection latency.

5.4.2 Comparison of Proposed Detector with State-of-the-Art

Table 5.5 compares the performances of the proposed detectors with several state-of-the-art seizure onset detectors. The detector in [28] uses the method of signal differentiation as a feature enhancement method but does not assume any form of channel selection. The detection algorithm in [40] extracts temporal and spectral features from iEEG channels. The spectral features of the iEEG are extracted by sliding one second intervals of the iEEG waveform through a filter bank and then it

Table 5.1: EEG-Based Detector Performance

Patient No.	EEG Sub-band Fusion Method	FA/hr	DL (sec)	Sensitivity (%)
1	AND	2	8.5	100
	OR	9.5	2	100
	MAJ	4	4.5	100
2	AND	5.5	3.5	100
	OR	6.75	2	100
	MAJ	5.75	3.25	100
3	AND	6.5	3.5	100
	OR	7	2	100
	MAJ	7	2	100
4	AND	3.75	1.56	100
	OR	8.75	0.22	100
	MAJ	4.75	0.5	100
5	AND	4	4	100
	OR	8	2	100
	MAJ	4	2	100
6	AND	5.5	2	100
	OR	5	0	100
	MAJ	2	1	100
7	AND	2.5	1.5	100
	OR	3.5	0	100
	MAJ	3.5	0.5	100
Avg	AND	4.3	3.5	100
	OR	3.5	1.2	100
	MAJ	4.4	2	100

measures the energy falling within the passband of each filter. The detector in [53] analyzes HRV using four different HRV methods with short term moving window analysis. In [12], ten time-domain and frequency-domain features are extracted from HRV and classified using an Artificial Neural Network (ANN). The detector in [36] is based on the fusion of HRV-based decision and EEG-based decision. The detector extracts time-domain features from HRV and spectral features from EEG to detect neonatal seizures. In [35], the fusion detector is based on two systems. In the first system, the features from HRV and EEG are combined and then classified, whereas in the second system, the independent decisions of the HRV and EEG data are combined to yield a decision. The second system outperformed the first system

Table 5.2: ECG-Based Detector Performance

Patient No.	FA/hr	DL (sec)	Sensitivity (%)
1	9.5	20.5	100
2	1.5	8.25	100
3	3	15	100
4	9	8	75
5	6	12	100
6	5	8	100
7	3.5	10	100
Avg	5.4	13.1	96.4

and its performance is depicted in Table 5.5. The detector in [43] is developed by NeuroPace Inc. and is commercially available. The detector in [44] is an FDA approved seizure onset detector developed by Optima Neuroscience. The proposed detectors in this chapter perform optimally in terms of sensitivity, specificity, and DL when compared with the existing detectors.

Table 5.3: EEG-ECG Direct Fusion Detector Performance

Patient No.	Fusion Type	FA/hr	DL (sec)	Sensitivity (%)
1	AND	0.5	26	100
	OR	3.5	17.5	100
	MAJ	3.5	17.5	100
2	AND	1.5	18.5	100
	OR	2.25	18.25	100
	MAJ	1.75	18.25	100
3	AND	0	19.5	100
	OR	2.5	15	100
	MAJ	1	15	100
4	AND	2.5	17.37	100
	OR	2.75	8.25	100
	MAJ	2.5	8.4	100
5	AND	1	20	100
	OR	3	12	100
	MAJ	2	12	100
6	AND	0	6	100
	OR	2	3	100
	MAJ	1	5	100
7	AND	0.5	12	100
	OR	1.5	10	100
	MAJ	1	10	100
Avg	AND	0.9	17.1	100
	OR	2.5	12	100
	MAJ	1.6	12.3	100

Table 5.4: Performance of the OF EEG-ECG Fusion Detector

Patient No.	Fusion Type	FA/hr	DL (sec)	Sensitivity (%)
1	AND	1	8.5	100
	OR	5	2	100
	MAJ	1.5	8	100
2	AND	5.5	4.5	100
	OR	6.75	2	100
	MAJ	5.75	3.25	100
3	AND	5.5	3	100
	OR	7	2.5	100
	MAJ	6.5	2.5	100
4	AND	3.5	2.1	100
	OR	5.5	0.3	100
	MAJ	3.5	0.4	100
5	AND	4	5	100
	OR	6	2	100
	MAJ	4	3	100
6	AND	1	2	100
	OR	4	0	100
	MAJ	1.5	1	100
7	AND	1	4.5	100
	OR	2.5	0	100
	MAJ	1.5	3	100
Avg	AND	3.1	4.2	100
	OR	5.3	1.3	100
	MAJ	3	2.6	100

Table 5.5: Comparison of Average Detector Performances

Detector Architecture		FA/hr	DL (sec)	Sensitivity (%)	Specificity (%)
Direct Fusion Detector	AND	0.9	17.1	100	99.97
	OR	2.5	12	100	99.92
	MAJ	1.6	10.8	100	99.95
Over-ride Fusion Detector	AND	3.1	4.2	100	99.91
	OR	5.3	1.3	100	99.84
	MAJ	3	2.6	100	99.91
[28]		0.125	9.2	89.8	n/a
[40]		0.6	5	97	n/a
[53]		n/a	14	76.64	n/a
[12]		n/a	n/a	88.66	90
[36]		3.96	n/a	97.52	n/a
[35]		n/a	n/a	95.2	94.3
[43]		0.013	5.01	97	n/a
[44]		0.086	n/a	80	n/a

6. FURTHER INVESTIGATIONS

In this chapter, additional work regarding seizure detection is presented. Specifically, a new measure for detecting seizures in EEG is investigated. Previously, energy was the main feature that was chosen to study the manifestation of epilepsy in EEG. In this chapter, we investigate neural synchrony as a means to detect the early onset of seizures in EEG. Experimental studies have shown that wide-spread synchronization plays a prominent role in normal brain activity, particularly in the dynamics of sleep and wakefulness [54]. However, uncontrollable spreading of synchronized rhythmicity over large regions of the brain has been directly related with the pathogenesis of some disorders of the central nervous system, particularly in epilepsy [55],[54].

6.1 Neural Synchronization Measurement

The neural synchronization feature studied in this chapter is based on calculating the condition number (CN) of the recorded EEG matrix at a particular time-instant. Neural synchronization calculation via the CN is a fast and simple method and has not been investigated previously for the purpose of determining the amount of neural synchronization in EEG signals.

The level of synchronization between the EEG channels is measured by calculating the CN of the EEG matrix. Let X denote an EEG matrix of size $M_{ch} \times J$, where M_{ch} denotes the number of EEG channels and J stands for the number of time samples of the EEG matrix. To calculate the CN of a patient's EEG record, a window of size $M_{ch} \times J$ is shifted along the EEG record by an interval of 1-second to extract the EEG epoch matrix X_T. The CN of X_T is the ratio of the maximum to the minimum

singular values of matrix X_T. In detail, the CN of X_T is given by

$$\kappa(X_T) = \frac{\sigma_{SV_{max}}}{\sigma_{SV_{min}}}, \tag{6.1}$$

where κ denotes the CN, $\sigma_{SV_{max}}$ is the maximum singular value of X_T, and $\sigma_{SV_{min}}$ is the minimum singular value of X_T. The singular values are computed using the singular value decomposition (SVD) such that

$$X_T = \Gamma \Sigma \Psi' \tag{6.2}$$

where Γ and Ψ are $M_{ch} \times M_{ch}$ and $J \times J$ orthonormal matrices, respectively, and Σ represents the $M_{ch} \times J$ diagonal matrix of singular values. Large values of κ indicate that the matrix at that time instant is ill-conditioned and the channels of the EEG are highly correlated, indicating epileptic activity. In other words, the CN is an indicator of whether or not the channels of the EEG matrix are highly synchronized. Large values of κ indicates hyper-synchronization between the channels of the EEG matrix at that time instant.

6.2 Seizure Detection via Neural Synchronization

We implement a seizure onset detection system based on the neural synchronization calculation method explained in Section 6.1. Figure 6.1 illustrates the components making up the neural synchronization based SOD. The classification unit (SVM and timing constraint unit) are similar to that described in Chapter2.

6.2.1 Performance of the CN-based SOD

In this section, the effectiveness of the proposed CN-based SOD is analyzed. The CN-based SOD is tested on the same clinical database mentioned in Section 3.1 and

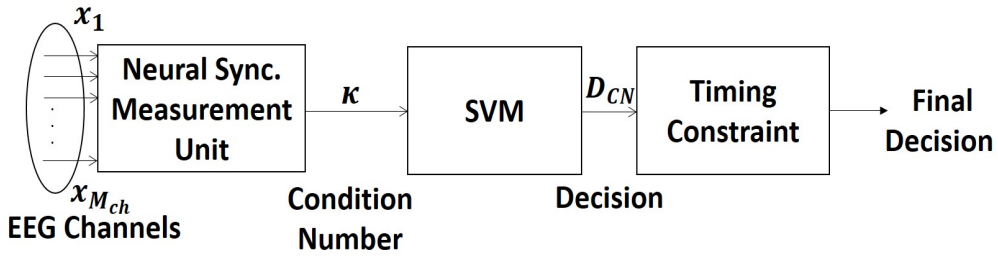

Figure 6.1: An illustration of the CN-based SOD.

the performance is discussed.

Figure 6.2 depicts the CN waveform for an hour long EEG recording of patient 1. Figure 6.3 shows the computed CN for a 2-hour EEG recording for patient 3. In both figures, the seizure instances, as specified by an expert, are highlighted in red while non-seizure instances are shown in blue. The figures also show a dramatic increase in the neural synchronization (large CN values) at the onset of the seizure. The amount of neural synchronization decreases towards the end of the seizure event. The results demonstrate the ability of the CN to accurately estimate the level of synchronization among the EEG channels and hence its applicability in epileptic seizure detection.

Table 6.1 shows the performance of the CN-based SOD for five patients. Neural synchrony via CN is a powerful tool in the detection of early seizure onset, as can be seen by the very low detection latency of 0.69 seconds. Also, the CN-based SOD achieves 100% sensitivity, showing a promising future for neural synchrony as a measure for seizure detection in EEG. The high false alarm rate observed can be a result of pre-seizure synchronization or IED before or after seizures. Still, the level of false alarms is high for applicability in seizure detection systems.

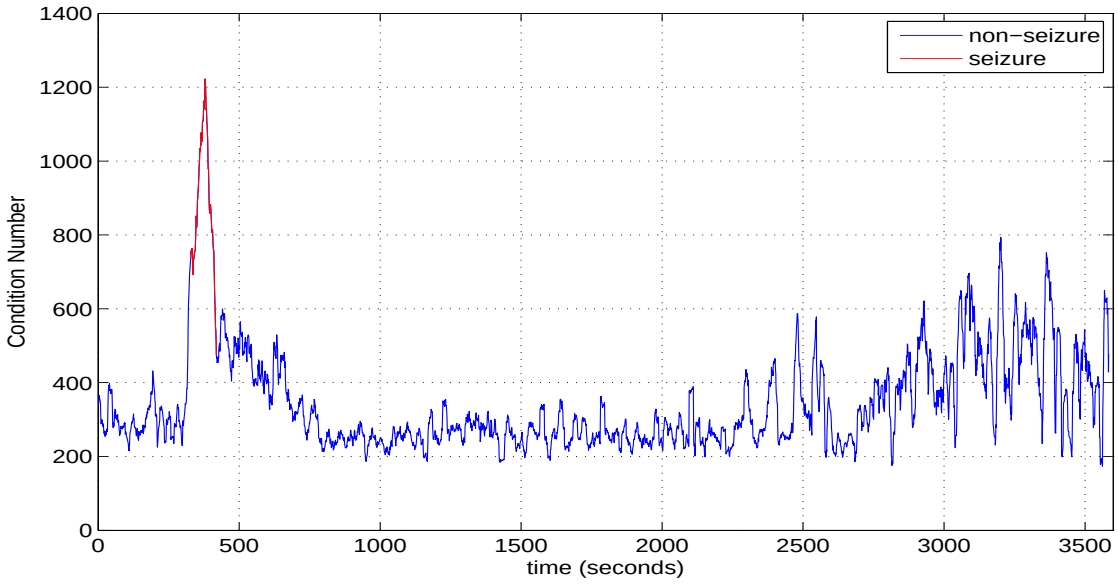

Figure 6.2: Condition number waveform for 1-hour of EEG recording for patient 1.

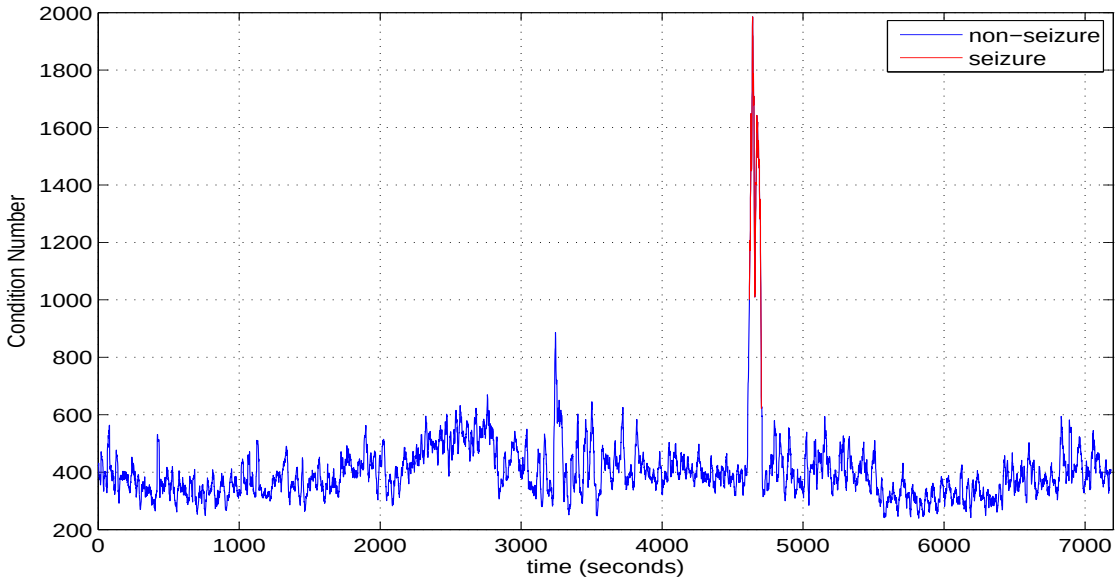

Figure 6.3: Condition number waveform for 2-hour of EEG recording for patient 3.

Table 6.1: CN-based Detector Performance

Patient	Sensitivity (%)	Detection Latency (sec)	FA / hr
1	100	0	11.6
2	100	0.16	14
3	100	2.8	7.1
4	100	0.2	12.4
5	100	0.3	8
Avg	**100**	**0.69**	**10.6**

6.3 Decision Fused Energy and Synchrony Based SOD

In an attempt to further improve the performance of SODs, we have conducted preliminary investigations in fusing synchrony and energy based seizure decisions to obtain a final detection decision. Figure 6.4 illustrates the detector architecture of the fused energy and neural synchrony based seizure onset detection system. The detector consists of the following stages: EEG energy detection unit (as given by the upper part of Figure 6.4), the neural synchronization detection unit (as given by the lower part of Figure 6.4), and the fusion unit. Specifically, the energy detection unit is composed of the EWSA, feature extraction, and classification stages. The neural synchronization detection unit is composed of condition number calculation and classification stages. The decisions obtained from the energy and neural synchronization detection units are then applied to the fusion unit to derive the detector's global decision.

The EWSA unit of the energy-based SOD is done in a similar manner to that explain in Section 3.2. Once the EWSA signal is obtained, the energy contained in the β, α, θ, and δ frequency bands is computed in the same manner as in Section 2.2.3. The classification unit is identical to that explained in Section 2.3.

In the fusion unit, the CN decision (d_{CN}) and the energy-based decision (d_E) are fused using two different techniques to obtain a single global decision. The first

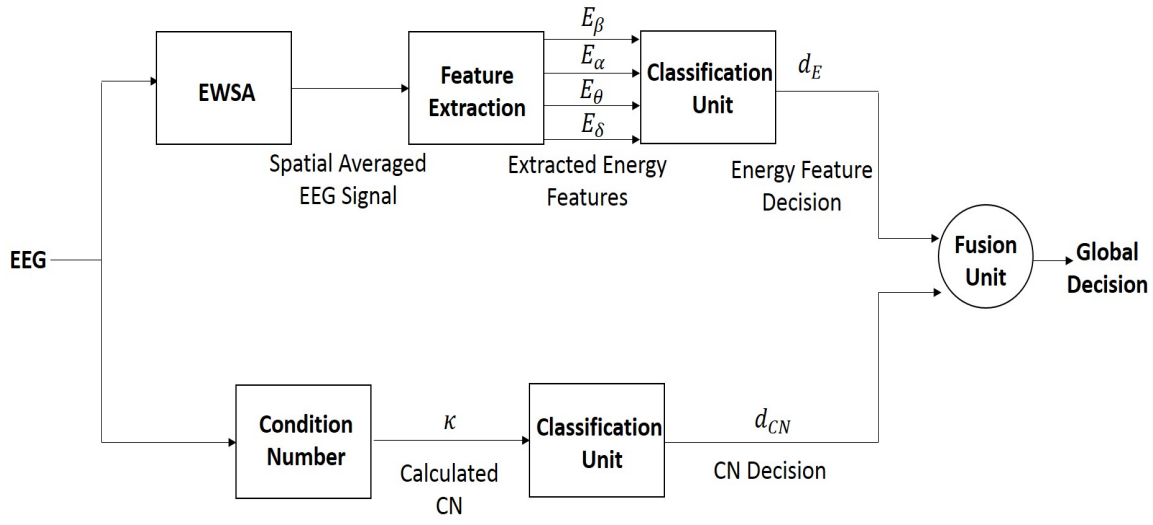

Figure 6.4: An illustration of the fused energy-based and neural synchrony-based SOD architecture.

fusion technique is based on the AND logical operator, where the d_{CN} and d_E must be classified as seizure for the global decision to yield a seizure result. Otherwise, the global result will be non-seizure. The second fusion technique is based on the OR logical operator. Here, the global decision declares a seizure event if at least one of the decisions (d_{CN} or d_E) yields a seizure event.

6.3.1 Performance Evaluation of Fused Energy and Synchrony Based SOD

Tables 6.2 and 6.3 show the performance results of the proposed detector under the AND and OR fusion technique, respectively. The detector has been tested on five different pediatric patients and was trained on 30 hours of continuous EEG records containing a total of 24 seizure instances and was tested on 6 hours of continuous EEG records that contain a total of six seizure instances. Analyzing each patient separately, it is evident that the OR fusion method yields the highest false alarm rate compared to the AND fusion technique. Such a performance is intuitive since

for the OR fusion technique, a global seizure event is declared if either d_{CN} or d_E is a seizure decision, whereas the AND method requires both features to be classified as a seizure before the detector can declare a seizure event. On the other hand, the OR method is able to detect the onset of a seizure in the shortest amount of time since this method is sensitive to any seizure alarm. Overall, both fusion techniques result in perfect sensitivity results.

Periods of high neural synchrony due to events not pertaining to seizure instances give rise to the high false alarm rates. Also, the high false alarm rates observed in the OR fusion technique is due to the energy-based SOD. This detector does not implement a feature enhancement unit, as we have proposed in Chapter 2. Therefore, non-seizure energy features are often misclassified as seizure features. The false detections of patient 4 are caused by non-physiological artifacts. All other false detections in the performance table are caused by periodic discharges that closely resemble the seizure onset of the subject. The false alarm rate can be improved by pre-processing the EEG waveform prior to feature extraction to rid the signal of artifacts and noise or by implementing a CSP-based feature enhancement unit in the energy-based SOD, as was done in Chapter 2.

Table 6.2: Detector Performance for AND Fusion

Patient	**Sensitivity (%)**	**Detection Latency (sec)**	**FA / hr**
1	100	1.67	6
2	100	1	3.5
3	100	5.8	1
4	100	0	2.7
5	100	6.7	0.62
Avg	**100**	**3.03**	**2.76**

Table 6.3: Detector Performance for OR Fusion

Patient	**Sensitivity (%)**	**Detection Latency (sec)**	**FA / hr**
A	100	0	16.5
B	100	0.25	17.75
C	100	0.6	8.8
D	100	0	8.25
E	100	0	9.12
Avg	**100**	**0.17**	**12.08**

7. CONCLUSION AND FUTURE WORK

In this chapter, we conclude the thesis with a summary of its goals and contributions followed by proposed improvements and directions for future work.

7.1 Goals and Contributions

The goal of this thesis was to design, evaluate, and clinically test the performance of a seizure onset detection system. Seizure detection systems are extremely beneficial and present a wide range of applications. For example, they could be used as warning devices to warn patients of oncoming seizures so that they take precaution and decrease or eliminate any unforeseen injury. SODs may also be used as therapeutic systems that are capable of detecting and reacting to the onset of a seizure and administering either anti-epileptic drugs or delivering an electrical stimulus to help decrease the effect of the seizure or eliminate it. Furthermore, knowledge that a reliable warning system is available may restore some individuals with the confidence and peace of mind that their condition has stolen from them.

In this thesis, we proposed three seizure detection systems, EEG-based SOD, ECG-based SOD, and a EEG-ECG fusion SOD. The SODs we developed contribute technically to the field of seizure detection in the following ways:

- **EEG Feature Enhancement Algorithm**: Chapter 2 presented a patient-specific seizure onset detector with two novel stages. The first proposed stage is an EEG feature enhancement stage which exploits the method of CSP to maximally differentiate between seizure and non-seizure EEG data. The differentiation between seizure and non-seizure EEG can be appreciated in Chapter 3 which shows that after CSP feature enhancement, extracted non-seizure energy features are attenuated while seizure energy features are significantly amplified.

The benefits of the proposed CSP feature enhancement method is clearly seen in the examples presented in Chapter 3 and in the performance of the detector.

- **Band-Sensitive Classification**: A novel band-sensitive classification system is also presented in Chapter 2. In this system, features are extracted from four seizure-relevant frequency sub-bands. These features are then classified independently by separate SVMs. The band-specific classification decisions are then fused to derive a global detection decision. The motivation behind the BS-classification system is that certain seizures portray unique electrographic alterations in specific frequencies, and analyzing each frequency sub-band separately allows for a deeper investigation of such manifestations. Additionally, for some patients, specific bands exhibit maximum separation between seizure and non-seizure events using the CSP-based feature enhancement stage. Investigating separate frequency bands enables an improved detection performance. This novel classification system can be appreciated by viewing the enhanced performance results, given in Chapter 3, versus the traditional classification system.

- **Time-Frequency Extracted HRV Features**: In Chapter 4, we introduced a ECG-based SOD that adopts a signal adaptive, quadratic time-frequency distribution approach in analyzing HRV based on the combination of the Matching-Pursuit and Wigner-Ville Distribution algorithm. Traditionally, HRV features have been analyzed using only time- and/or frequency-domain features which limits the information that is extracted from HRV. Because HRV is a non-linear and non-stationary signal, analyzing it via the MP-WVD enables better and more valuable feature extraction.

- **Use Multiple Biosignals**: Chapter 5 illustrated how the detectors presented

in Chapters 2 and 4 can be fused into a single detector. The EEG-ECG fused SOD provides benefits that a stand-alone EEG or ECG based detector may lack. The proposed fusion detector is equipped with two fusion techniques to combat noise that may hinder its performance. Clinical performance shows improved results versus stand-alone systems and state-of-the-art detectors.

- **Enhanced Detection Performance**: The detectors presented in this thesis have outperformed state-of-the-art detectors. The BS-EEG detector with CSP-enhanced features achieves a sensitivity of 100%, detection latency of 7.28 seconds, and 1.2 false alarm rate per hour for the MAJORITY fusion method and when combined with the ECG-detector presented in Chapter 4, a sensitivity of 100%, detection latency of 2.6 seconds, and a specificity of 99.91% for the MAJ fusion case is observed.

- **Neural Synchronization as a Detection Measure**: This thesis also investigated neural synchrony as a possible measure for the early detection of seizure via EEG. Chapter 6 presented a novel method to measure the amount of neural synchrony that exists between the EEG-channels at a particular time instant. The method is adopted into a seizure detection system and fused with an energy-based seizure detector. The results show a promising future for the use of neural synchrony based on the calculation of the CN of multi-channel EEG data as an effective measure for seizure detection. Specifically, the fused synchrony and energy-based detector achieves 100% sensitivity, a detection latency of 3.03 seconds, and a FA rate of 2.76 per hour.

7.2 Future Work

This section outlines possible future research directions to extend further the results of this thesis.

7.2.1 Automatic Noise Removal

The work done in this thesis does not implement any noise and artifact removal algorithm. Instead, our approach to deal with artifacts is based on training our detector to recognize artifacts, rather than actively removing them using standard signal processing techniques. In an attempt to further enhance our detectors' performances, several forms of EEG and ECG pre-processing techniques will be investigated.

7.2.2 Combined Energy and Neural Synchrony Features

All the fusion detectors implemented this thesis are based on the fusion of decisions made from independent detectors. A future direction is to combine neural synchrony based features and energy based features in a single feature vector and then apply a classification algorithm for a decision. EEG-ECG feature-based fusion will be investigated and compared with the decision based fusion. The goal of this research will be to investigate whether feature-based fusion improves the latency, sensitivity, or specificity of the detectors presented in this thesis.

7.2.3 Detecting Seizure Cessation

The goal of the detectors presented thus far was to indicate the onset of a seizure, but do not signal the end of a seizure. Detection of the cessation of a seizure allows for the automatic computation of the seizure duration and the duration from the end of one seizure to the beginning of the next. These quantities have clinical significance for neurologists. For instance, seizures that persist for more than ten minutes or seizures that are clustered close to each other may indicate a possible transition to a condition of status epilepticus. Status epilepticus refers to a life-threatening condition in which the brain enters a state of persistent seizure activity. Therefore, future work will investigate whether the transition from a seizure state back to a

non-seizure state can be learned using similar methods studied in this work.

7.2.4 Using Pre-Seizure Abnormalities to Enhance Seizure Detection

The EEG of some epileptic individuals exhibits patient-specific abnormalities prior to the electrographic onset of the seizure. These pre-seizure abnormalities may or may not resemble the electrographic signature of the onset. A detector that can recognize this patient-specific pre-seizure activity as well as estimate the time duration (from training data) between the pre-seizure activity and the onset of the seizure can be of great use as an effective warning device. Several challenges are faced when trying to detect abnormal pre-seizure electrographic changes since the time between the beginning of pre-seizure activity and the actual onset is variable. Also, the abnormal EEG activity can be very heterogeneous itself. However, successful identification of pre-seizure activity will enable powerful seizure *prediction* systems.

REFERENCES

[1] A. Varsavsky, I. Mareels, and M. Cook, *Epileptic Seizures and the EEG: Measurement, Models, Detection, and Prediction*, CRC Press, 2010.

[2] J. Engel, *Seizures and epilepsy*, Oxford University Press, 2013.

[3] Z. Haneef and A. Maheshwari, *A Concise Manual of Epilepsy*, Neurogroups Publications, 2015.

[4] K. Laxer, E. Trinka, L. Hirsch, F. Cendes, J. Langfitt, N. Delanty, T. Resnick, and S. Benbadis, "The consequences of refractory epilepsy and its treatment," *Epilepsy and Behavior*, vol. 37, pp. 59-70, 2014.

[5] *Electroencephalography*, 2016. [Online]. Available: `http://www.bem.fi/book/13/13.htm`.

[6] Hopkinsmedicine.org, "Electroencephalogram (EEG) Johns Hopkins Medicine Health Library," 2016. [Online]. Available: `http://www.hopkinsmedicine.org/healthlibrary/test_procedures/neurological/electroencephalogram_eeg_92,p07655/`.

[7] S. Sanei and J. Chambers, *EEG Signal Processing*, John Wiley & Sons, 2008.

[8] Frequencies.ssrc.org, "Thought-waves — frequencies", 2012. [Online]. Available: `http://frequencies.ssrc.org/2012/01/13/thought-waves/`.

[9] Almostadoctor, "Understanding ECGs", 2009. [Online]. Available: `http://almostadoctor.co.uk/content/systems/-cardiovascular-system/ecgs/understanding-ecgs`.

[10] Life Breath, "Resting ECG", 2016. [Online]. Available: `http://www.lifebreath.org/diagnostic-testing/resting-ecg`.

[11] K. Schiecke, M. Wacker, D. Piper, F. Benninger, M. Feucht, and H. Witte, "Advantages of signal-adaptive approaches for the nonlinear, time-variant analysis of heart rate variability of children with temporal lobe epilepsy", *Annual International Conference of the IEEE Engineering in Medicine and Biology Society*, 2014.

[12] S. Behbahani, N. Dabanloo, A. Nasrabadi, C. Teixeira, and A. Dourado, "A new algorithm for detection of epileptic seizures based on HRV signal," *Journal of Experimental & Theoretical Artificial Intelligence*, vol. 26, no. 6, pp. 251-265, 2014.

[13] C. Sevcencu and J. Struijk, "Autonomic alterations and cardiac changes in epilepsy," *Epilepsia*, vol. 51, no. 5, pp. 725-737, 2010.

[14] V. Prasad, D. Kendrick, K. Sayal, S. Thomas, and J. West, "Injury among children and young adults with epilepsy," *Pediatrics*, vol. 133, no. 5, pp. 827-835, 2014.

[15] A. Van de Val, K. Cuppens, B. Bonroy, M. Milosevic, K. Jansen, S. Van Huffel, B. Vanrumste, L. Lagae, and B. Ceulemans, "Non-EEG seizure-detection systems and potential SUDEP prevention: state of the art," *Seizure*, vol. 22, no. 5, pp. 345-355, 2013.

[16] A. Shoeb, H. Edwards, J. Connolly, B. Bourgeois, S. T. Treves, and J. Guttag, "Patient-specific seizure onset detection," *Epilepsy & Behavior*, vol. 5, no. 4, pp. 483-498, 2004.

[17] J. Gotman and P. Gloor, "Automatic recognition and quantification of interictal epileptic activity in the human scalp EEG," *Electroencephalography and clinical Neurophysiology*, vol. 41, no. 5, pp. 513-529, 1976.

[18] L. Meng, M. G. Frei, I. Osorio, G. Strang, and T. Q. Nguyen, "Gaussian mixture models of ECoG signal features for improved detection of epileptic seizures," *Medical Engineering & Physics*, vol. 26, no. 5, pp. 379-393, 2004.

[19] K. Fu, J. Qu, Y. Chai, and T. Zou, "Hilbert marginal spectrum analysis for automatic seizure detection in EEG signals," *Biomedical Signal Processing and Control*, vol 18, pp. 179-185, 2015.

[20] A. Correa, L. Orosco, P. Diez, and E. Laciar, "Automatic detection of epileptic seizure in long-term EEG records, *Computers in biology and medicine*, vol 57. pp. 66-73, 2015.

[21] A. Shoeb and J. Guttang, "Application of machine learning to epileptic seizure detection," *Proceedings of the 27th International Conference on Machine Learning (ICML-10)*, pp. 975-982, 2010.

[22] S. Yuan, W. Zhou, Q. Yuan, Y. Zhang, and Q. Meng, "Automatic seizure detection using diffusion distance and BLDA in intracranial EEG," *Epilepsy and Behavior*, vol. 31, pp. 339-345, 2014.

[23] Q. Yuan, W. Zhou, Y. Liu, and J. Wang, "Epileptic seizure detection iwth linear and nonlinear features," *Epilepsy and Behavior*, vol. 24, pp. 415-421, 2012.

[24] K. Gadhoumi, L. Jean-Marc, and J. Gotman, "Seizure prediction in patients with mesial temporal lobe epilepsy using EEG measures of state similarity," *Clinical Neurophysiology*, vol. 124, no. 9, pp. 1745-1754, 2013.

[25] G. R. Minasyan, J. B. Chatten, M. J. Chatten, and R. N. Harner, "Patient-specific early seizure detection from scalp eeg," *Journal of clinical neurophysiology: official publication of the American Electroencephalographic Society*, vol. 27, no. 3, pp. 163, 2010.

[26] M. Z. Parvez, and P. Manoranjan, "Epileptic Seizure Detection by Analyzing EEG Signals using Different Transformation Techniques." *Neurocomputing*, vol. 145, pp. 190-200, 2014.

[27] S. Li, W. Zhou, Q. Yuan, and Y. Liu, "Seizure Prediction Using Spike Rate of Intracranial EEG," *IEEE Transactions on Neural Systems and Rehabilitation Engineering*, vol. 21, no. 6, pp. 880-886, 2013.

[28] K. K. Majumdar and P. Vardhan, "Automatic seizure detection in ECoG by differential operator and windowed variance," *IEEE Transactions on Neural Systems and Rehabilitation Engineering*, vol. 19, no. 4, pp. 356-365, 2011.

[29] S. Samadi, L. Amini, H. Soltanian-Zadeh, and C. Jutten, "Identification of brain regions involved in epilepsy using common spatial pattern," *Statistical signal Processing Workshop*", pp. 825-828, 2011.

[30] Y. Wang, S. Gao, and X. Gao, "Common spatial pattern method for channel selection in motor imagery based brain-computer interface," *27th Annual International Conference of Engineering in Medicine and Biology Society*, pp. 5392-5395, 2006.

[31] H. Ramoser, J. Muller-Gerking, and G. Pfurtscheller, "Optimal spatial filtering of single trial EEG during imagined hand movement," *IEEE Transactions on Rehabilitation Engineering*, vo. 8, no. 4, pp. 447-456, 2000.

[32] J. Duun-Henriksen, T. W. Kjaer, R. E. Madsen, L. S. Remvig, C. E. Thomsen, and H. B. D. Sorensen, "Channel selection for automatic seizure detection," *Clinical Neurophysiology*, vol. 123, no. 1, pp. 84-92, 2012.

[33] S. Behbahani, N. Dabanloo, A. Nasrabadi, C. Teixeira, A. Dourado, "Pre-ictal heart rate variability assessment of epileptic seizures by means of linear and non-

linear analyses," *Anadolu Kardiyol Derg*, vol. 13, no. 8, pp. 797-803, 2013.

[34] K. Schiecke, M. Wacker, D. Piper, F. Benninger, M. Feucht, and H. Witte, "Time-variant, frequency-selective, linear and nonlinear analysis of heart rate variability in children with temporal lobe epilepsy," *IEEE Transactions on Biomedical Engineering*, vol. 61, no. 6, pp. 1798-1808, 2014.

[35] M. Mesbah, M. Balakrishnan, P. Colditz, and B. Boashash, "Automatic seizure detection based on the combination of newborn multi-channel EEG and HRV information," *EURASIP Journal on Advances in Signal Processing*, no. 1, pp. 1-14, 2012.

[36] B. Greene, G. Boylan, R. Reilly, P. Chazal, and S. Connolly, "Combination of EEG and ECG for improved automatic neonatal seizure detection," *Clinical neurophysiology*, vol 118, no. 6, pp. 1348-1359, 2007.

[37] B. Boashash, "Estimating and interpreting the instantaneous frequency of a signal I. Fundamentals," *Proceedings of the IEEE*, vol. 80, no. 4, pp. 520-538, 1992.

[38] G. Strang and T. Nguyen, *Wavelets and filter banks*, SIAM, 1996.

[39] A. L. Goldberger, L. AN. Amaral, L. Glass, J. M. Hausdorff, P. Ch. Ivanov, R.G. Mark, J. E. Mietus, G. B. Moody, C. K. Peng, and H. E. Stanley, "Physiobank, physiotoolkit, and physionet components of a new research resource for complex physiologic signals," *Circulation*, vol. 101, no. 23, pp. 215-220, 2000.

[40] A. Kharbouch, A. Shoeb, J. Guttag, and S. S. Cash, "An algorithm for seizure onset detection using intracranial EEG," *Epilepsy & Behavior*, vol. 22, pp. S29-S35, 2011.

[41] J. Rasekhi, M.R. K. Mollaei, M. Bandarabadi, C. A. Teixeira, and A. Dourado, "Preprocessing effects of 22 linear univariate features on the performance of seizure prediction methods," *Journal of neuroscience methods*, vol. 217, no. 1, pp. 9-16, 2013.

[42] N. Moghim and D. W. Corne, "Predicting Epileptic Seizures in Advance," *PloS one*, vol. 9, no. 6, 2014.

[43] A. Gardner, *A novelty detection approach to seizure analysis from intracranical EEG*, PhD Doctor Dissertation, Georgia Institute of Technology, 2004.

[44] I. Osorio, H. P. Zaveri, M. G. Frei, S. Arthurs, *Epilepsy: The Intersection of Neurosciences, Biology Mathematics Engineering, and Physics*, CRC Press, 2011.

[45] X. Ning, I.W. Selesnick, and L. Duval, "Chromatogram baseline estimation and denoising using sparsity (BEADS)," *Chemometrics and Intelligent Laboratory Systems*, vol 139, pp. 156-167, 2014.

[46] M. Mesbah, B. Boashash, M. Balakrishnan, and P. Cldiz, "Heart rate variability time-frequency analysis for newborn seizure detection," *Advanced Biosignal Processing*, Springer Berlin Heidelberg, pp. 95-121, 2009.

[47] L. Mainardi, "On the quantification of heart rate variabiliy spectral parameters using time-frequency and time-varying methods," *Philosophical Transactions of The Royal Society*, vol. 367, pp. 255-275, 2008.

[48] M. Wacker and H. Witte, "Time-frequency techniques in biomedical signal analysis," *Methods Inf Med*, vol.. 52, no. 4, pp. 279-296, 2013.

[49] F. Lucena, A. Cavalcante, Y. Takeuchi, A. Barros, and N. Ohnishi, "Wavelet entropy measure based on matching pursuit decomposition and its analysis to heart-

beat intervals," *Neural Information Processing, Theory and Algorithms*, Springer Berlin Heidelberg, pp. 503-511, 2010.

[50] L. Boubchir, S. Al-Maadeed, and A. Bouridane, "On the use of time-frequency features for detecting and classifying epileptic seizure activities in non-stationary EEG signals," *IEEE International Conference on Acoustics, Speech and Signal Processing*, 2014.

[51] M. Ihle, H. Feldwisch-Drentrup, C.A., Teizeira, A., Witon, B. Schelter, J. Timmer, and A. Schulze-Bonhage, "EPILEPSIAEA European epilepsy database," *Computer methods and programs in biomedicine*, vol 106, no3, pp. 127-138, 2012.

[52] M. Hirsch, D.M. Altenmuller, and A Schulze-Bonhage, "Latencies from intracranial seizure onset to ictal tachycardia: A comparison to surface EEG patterns and other clinical signs," *Epilepsia*, vol. 56, no. 10, pp. 1639-1647, 2014.

[53] J. Jeppesen, S. Benickzky, P. Sidenius, and A. Fuglsang-Frederiksen, "Detection of epileptic seizures with a modified heart rate variability algorithm based on Lorenz plot," *Seizure*, vol. 24, pp. 1-7, 2015.

[54] V. Shusterman and W. C. Troy, "From baseline to pileptiform activity: a path to synchronized rhythmicity in large-scale neural networks," *Physical Review*, vol. 77, no. 6, 2008.

[55] J. Milton and P. Jung, *Epilepsy as a Dynamic Disease,* Biological and medical physics series, Springer, 2003.